THE OHIO STATE UNIVERSITY

Electrical Conductivity of Ion Implanted Ladder and Semi-Ladder Polymers

Arthur J. Epstein
Department of Physics

Air Force Office of Scientific Research
Bolling Air Force Base, D.C. 20332-6448

92-C-0002
Contract No. F49620-[redacted]
Final Report

July 1993

REPORT DOCUMENTATION PAGE

1. AGENCY USE ONLY (Leave blank)	2. REPORT DATE	3. REPORT TYPE AND DATES COVERED
	7/2/93	Final 11/1/91 - 12/31/92

4. TITLE AND SUBTITLE

Electrical Conductivity of Ion Implanted Ladder and Semi-Ladder Polymers

62102F 2419 00

6. AUTHOR(S)

Arthur J. Epstein

7. PERFORMING ORGANIZATION NAME(S) AND ADDRESS(ES)

The Ohio State University
1314 Kinnear Road
Columbus, OH 43212-1194

8. PERFORMING ORGANIZATION REPORT NUMBER

9. SPONSORING/MONITORING AGENCY NAME(S) AND ADDRESS(ES)

AFOSR/NC
Building 410, Bolling AFB DC
20332-6448

10. SPONSORING/MONITORING AGENCY REPORT NUMBER

93-C 0062
F49620-~~90-C-0079~~

11. SUPPLEMENTARY NOTES

12a. DISTRIBUTION/AVAILABILITY STATEMENT

APPROVED FOR PUBLIC RELEASE: Distribution is unlimited

13. ABSTRACT (Maximum 200 words)

Aromatic heterocyclic ordered rigid rod, ladder and semi-ladder polymers (including BBL, PBO, PBT, and BBB) combine exceptional high temperature stability with excellent mechanical properties as well as environmental stability. We have continued our systematic study of the electronic, photonic, and environmental properties of the pristine polymer. We have discovered the presence of a significant photoconductivity in PBO and characterized its photoluminescence. Extending our photoinduced absorption spectroscopy studies to the millisecond regime we have found the presence of two weak photoinduced optical absorptions. The difference in behavior as compared to other conjugated polymers likely reflects the increased order in the pristine rigid rod and ladder polymers. We have extended our temperature dependent charge transport (dc conductivity, microwave frequency conductivity and dielectric constant, thermoelectric power, magnetoconductivity and electron spin resonance) studies of the ion implanted polymers as a function of implantation dosage. A nonmetal-to-metal transition is found as a function of increasing dosage (occurring at 4×10^{16} ions/cm^2). For implanted samples of metallic behavior, a unique transition to a nonmetallic behavior has been discovered at 30K. The origin of this transition is attributed to the opening up of a Coulomb gap.

14. SUBJECT TERMS

55

17. SECURITY CLASSIFICATION OF REPORT	18. SECURITY CLASSIFICATION OF THIS PAGE	19. SECURITY CLASSIFICATION OF ABSTRACT	20. LIMITATION OF ABSTRACT
Unclassified	Unclassified	Unclassified	UL (Unlimited) SAR (Same As Report

THE OHIO STATE UNIVERSITY

Electrical Conductivity of Ion Implanted Ladder and Semi-Ladder Polymers

Arthur J. Epstein
Department of Physics

Air Force Office of Scientific Research
Bolling Air Force Base, D.C. 20332-6448

92-C-0002
Contract No. F49620-[redacted]
Final Report
RF Project No. 768616/724007

July 1993

FINAL TECHNICAL REPORT FOR
AFOSR CONTRACT F49620--90-C-0072
1 NOVEMBER 1991 - 31 DECEMBER 1992

Abstract

Aromatic heterocyclic ordered rigid rod, ladder and semi-ladder polymers (including BBL, PBO, PBT, and BBB) combine exceptional high temperature stability with excellent mechanical properties as well as environmental stability. We have continued our systematic study of the electronic, photonic, and environmental properties of the pristine polymer. We have discovered the presence of a significant photoconductivity in PBO and characterized its photoluminescence. Extending our photoinduced absorption spectroscopy studies to the millisecond regime we have found the presence of two weak photoinduced optical absorptions. The difference in behavior as compared to other conjugated polymers likely reflects the increased order in the pristine rigid rod and ladder polymers. We have extended our temperature dependent charge transport (dc conductivity, microwave frequency conductivity and dielectric constant, thermoelectric power, magnetoconductivity and electron spin resonance) studies of the ion implanted polymers as a function of implantation dosage. A nonmetal-to-metal transition is found as a function of increasing dosage (occurring at 4×10^{16} ions/cm^2). For implanted samples of metallic behavior, a unique transition to a nonmetallic behavior has been discovered at 30K. The origin of this transition is attributed to the opening up of a Coulomb gap.

TABLE OF CONTENTS

LIST OF FIGURES AND TABLES

I. BACKGROUND AND OBJECTIVES

Aromatic heterocyclic ordered rigid rod, ladder, and semi-ladder polymers, exemplified by poly(1,4-phenylene-2, 6-benzobisthiazole) PBT), poly(1,4-phenylene-2, 6-benzobisoxazole) PBO), poly(2,5-dihydroxy-1,4-phenylene-2, 6-benzobisthiazole) (DHPBT), poly(2,5-dihydroxy-1, 4-phenylene-2, 6-benzobisoxazole) (DHPBO), benzimidazobenzophenanthroline-type ladder (BBL) and semi-ladder (BBB) polymers, combine exceptional high temperature stability (500-700°C) with excellent mechanical properties and environmental (chemical and photochemical) resistance[1-12]. This combination of properties makes these polymers suitable for many applications, including aircraft and aerospace, high strength fibers, molecular composites, engineering structures, and heat-resistance coatings.[8-11] This class of high performance organic materials has emerged from many years of work under the Air Force Ordered Polymer research program.[8,9] Figure 1 shows the repeat unit for BBB, BBL, PBT, DHPBO, DHPBT and PBO polymers.

In contrast to the effects of ion implantation in sigma bonded polymers (where conductivities at room temperature of order 10^{-1} S/cm result[13,14]) ion implantation of rigid rod and ladder polymers results in a three orders of magnitude larger conductivity of ~10^2 S/cm with some samples[15] having conductivity at room temperature as high as 220 S/cm. These highly conducting, environmentally stable polymers provide an attractive candidates for Air Force and Department of Defense future technologies.

During the first contract year we carried out extensive surface analytical studies of the ion implanted polymers in comparison to the pristine polymers. The results of X-ray photoemission spectroscopy, scanning electron microscopy, and optical spectroscopy supported that the ion implantation resulted in the destruction of the one-dimensional pristine polymer structure and the formation of a three-dimensional carbon (graphite-like) disordered network. In particular, XPS of the implanted films showed a substantial reduction (and in many cases elimination) of heteroatom peaks leaving essentially only carbon. Figure 2 illustrates the contrast between pristine and ion implanted PBO. The optical spectrum of the ion implanted polymer reflects the elimination of the pristine polymer band structure and the formation of a

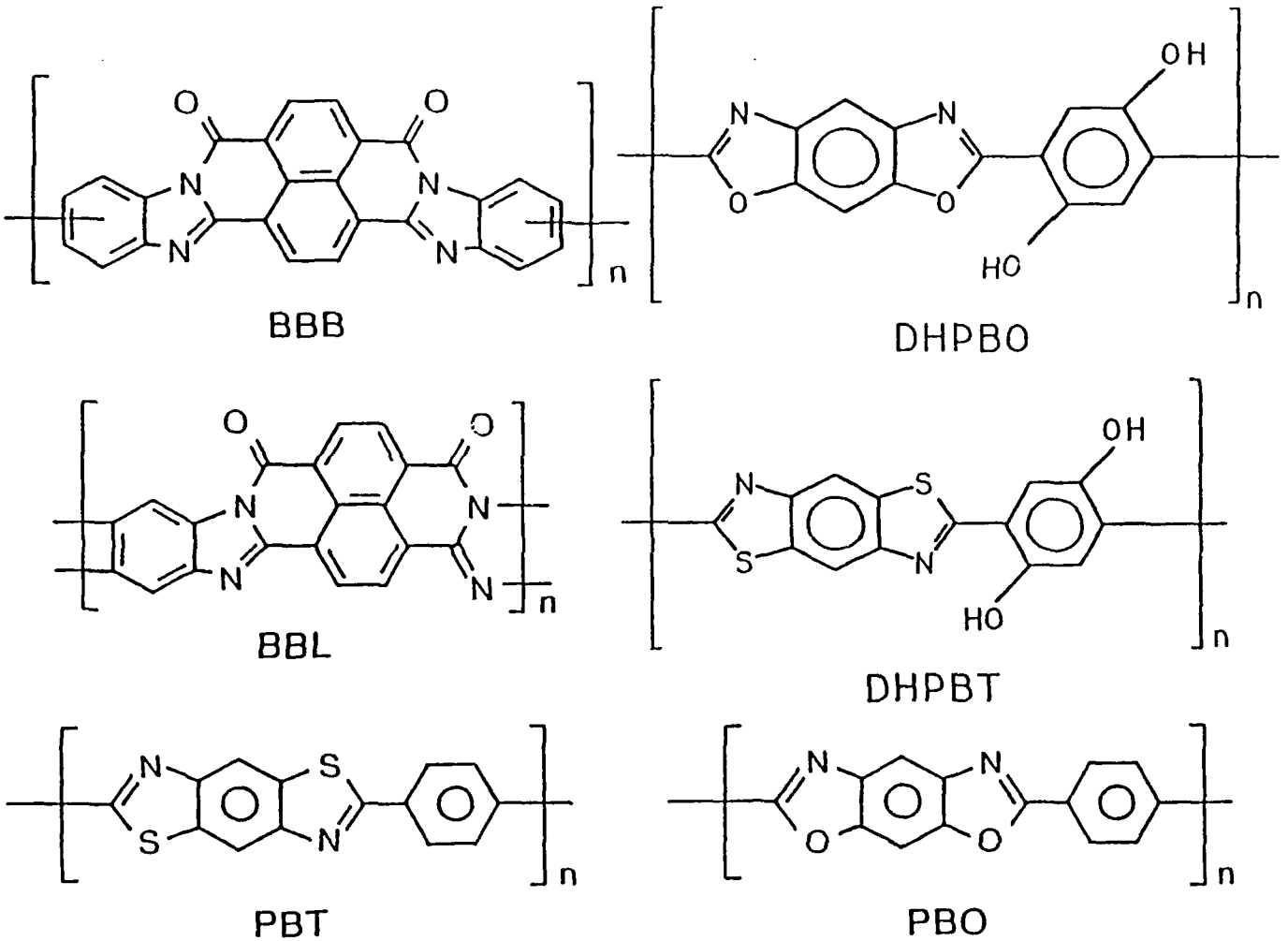

Figure 1 Molecular structures of rigid rod, ladder, and semi-ladder polymers: PBO, PBT, BBL, BBB, DHPBO, and DHPBT.

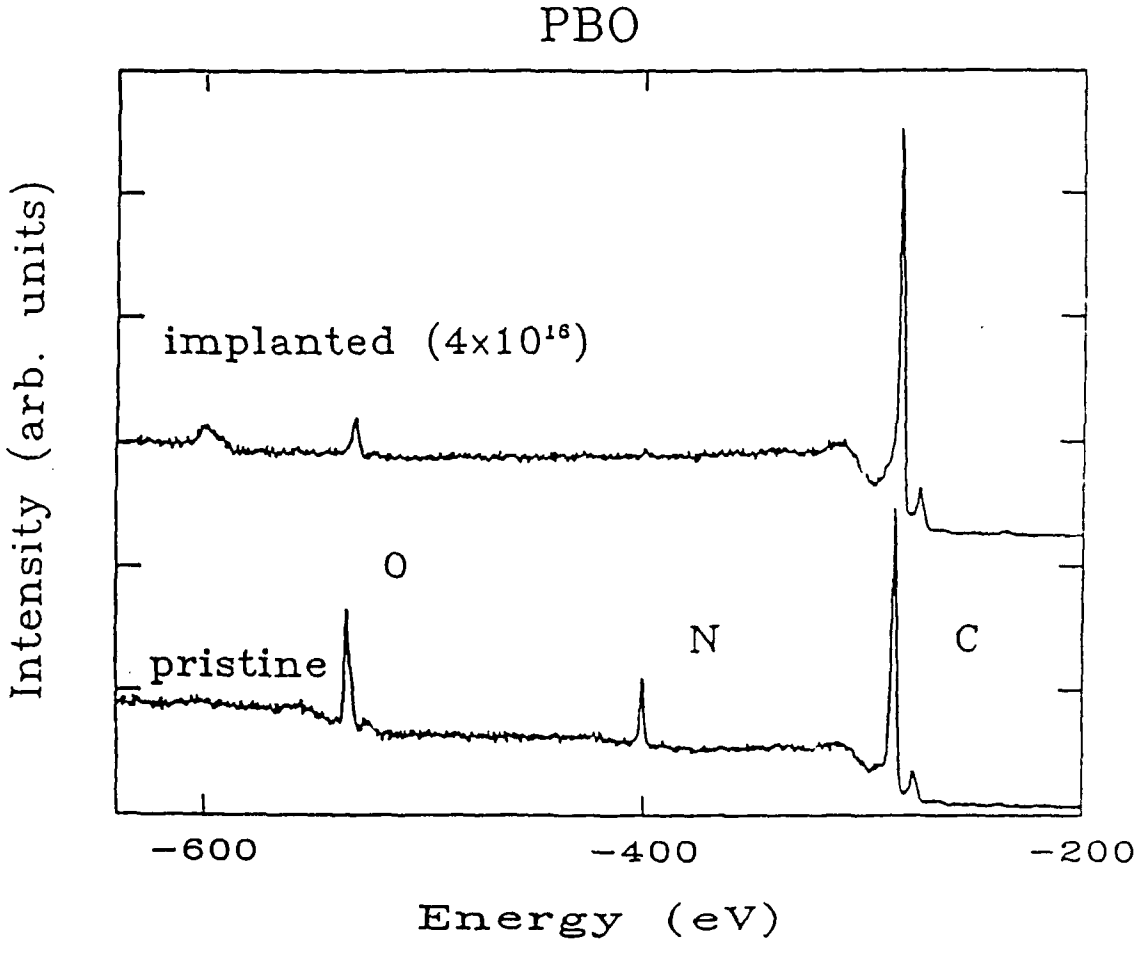

Figure 2 XPS spectra of pristine and 4 x 10^{16} ions/cm^2 implanted PBO.

wide metal-like band with a featureless transmission spectrum extending from the infrared through to the ultraviolet, Figure 3. As a result of the first year studies it was clear that the ion implantation technique enabled the formation of highly conducting surface layers on strong high temperature rigid rod and ladder polymers. Temperature dependent audio frequency conductivity and dielectric constant studies (10 - 10^5 Hz) showed that charge motion in the insulating rigid rod and ladder polymers is similar to that of other insulating polymers. However, initial attempts at long lived photoinduced absorption studies suggested that the photoinduced carriers may be more weakly localized than in less ordered polymers.

The objectives of this (the second year) research program (1 November 1991 -31 December 1992) were the elucidation of the electronic structure of ion implanted ladder, semi-ladder and rigid-rod polymers and a further determination of charge transport mechanisms. As part of this effort, photoinduced optical absorption conductivity and photoconductivity studies as well as electron paramagnetic resonance studies were carried out for the pristine rigid rod and ladder polymers. Models for the behavior in these materials were developed. Preliminary photoluminescence studies were performed and initial fabrication of electroluminescence devices incorporating the ion implanted regions as electrodes was attempted. DC conductivity, microwave frequency conductivity, microwave frequency dielectric constant, magnetoresistance, and thermopower studies were carried out on ion-implanted rigid rod and ladder polymers as a function of ion implantation dosage. Models were developed to describe the charge transport mechanisms of these materials as functions of temperature and ion implantation dosage.

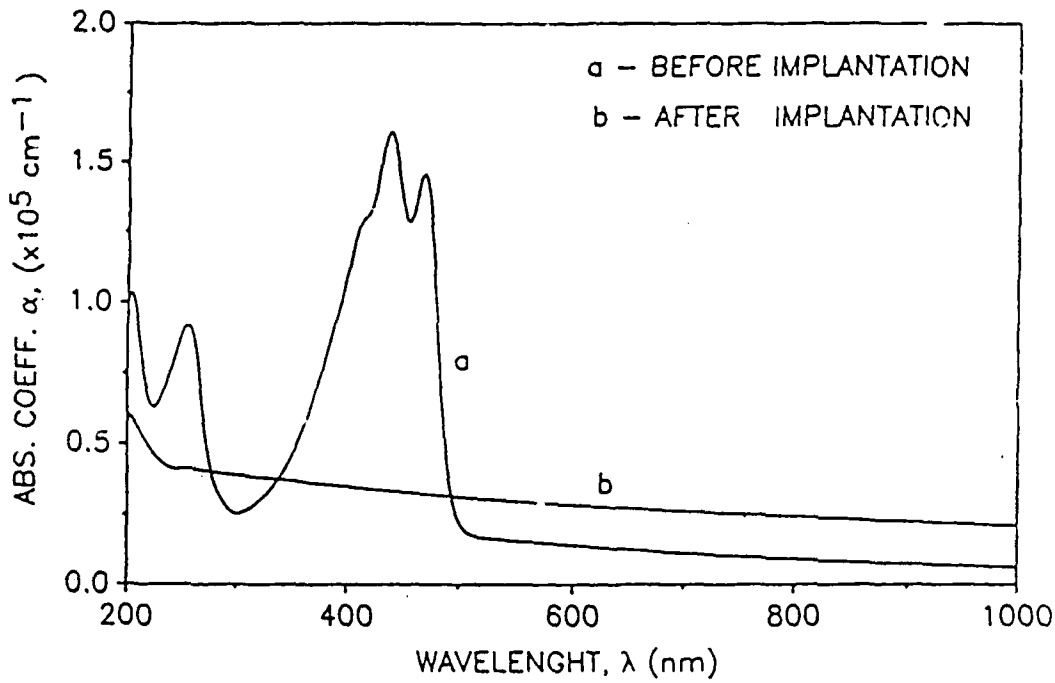

Figure 3 Optical spectra of pristine and 4 x 10^{16} ions/cm^2 implanted PBO.

II. RESULTS OF CONTRACT (1 NOVEMBER 1991 - 31 DECEMBER 1992)

Activities during this period are divided into studies of the pristine polymers and of the ion implanted polymers.

II.A. Pristine Rigid Rod and Ladder Polymer Studies

II.A.i. Photoinduced Absorption Studies

During the period of the contract we extended our OSU studies of photoinduced absorption of rigid rod and ladder polymers. Our earlier photoinduced infrared studies suggested that upon absorption of light of energy greater that the band gap that the rigid rod polymers (PBT) formed some modestly long lived intragap charged defect states (likely polarons). Figure 4a extends the earlier PBT data to 6000 cm^{-1} and contrasts the photoinduced signal with the direct infrared induced absorptions and heating induced (HI) effects. A broad photoinduced level centered at ~ 2900 cm^{-1} is clearly visible to together with associated active vibrations. Figure 4b represents the photoinduced absorption (to 6000 cm^{-1}) of PBO and contrasts it with the direct infrared absorption of the material. A photoinduced feature is seen now shifted down in energy so that it is centered at ~ 2000 cm^{-1}. No intragap levels were detected for the ladder polymers. The relative weak binding of the polaron levels in PBO and their absence in BBL and BBB contrasts with the usual behavior of conjugated polymers such as polythiophene, polyacetylene, and polyaniline. The origin of this anomalous behavior may lie in the greater order present in the rigid-rod and ladder polymers. Recent calculations by E.M. Conwell[16] and also P. Vogl and D.K. Campbell[17] suggest that in the presence of increased interchain coupling, polarons may be destabilized in favor of only weakly localized or even delocalized electrons and holes. Also, by implication, the polaron exciton would be destabilized in favor of a three-dimensional bound electron-hole exciton. It is speculated that this may improve the efficiency of photoluminescence and also electroluminescence. Recent studies of photoexcitations in polyphenylenevinylene prepared with differing degrees of local order suggest that the increased local order improves the electroluminescence efficiency.[18]

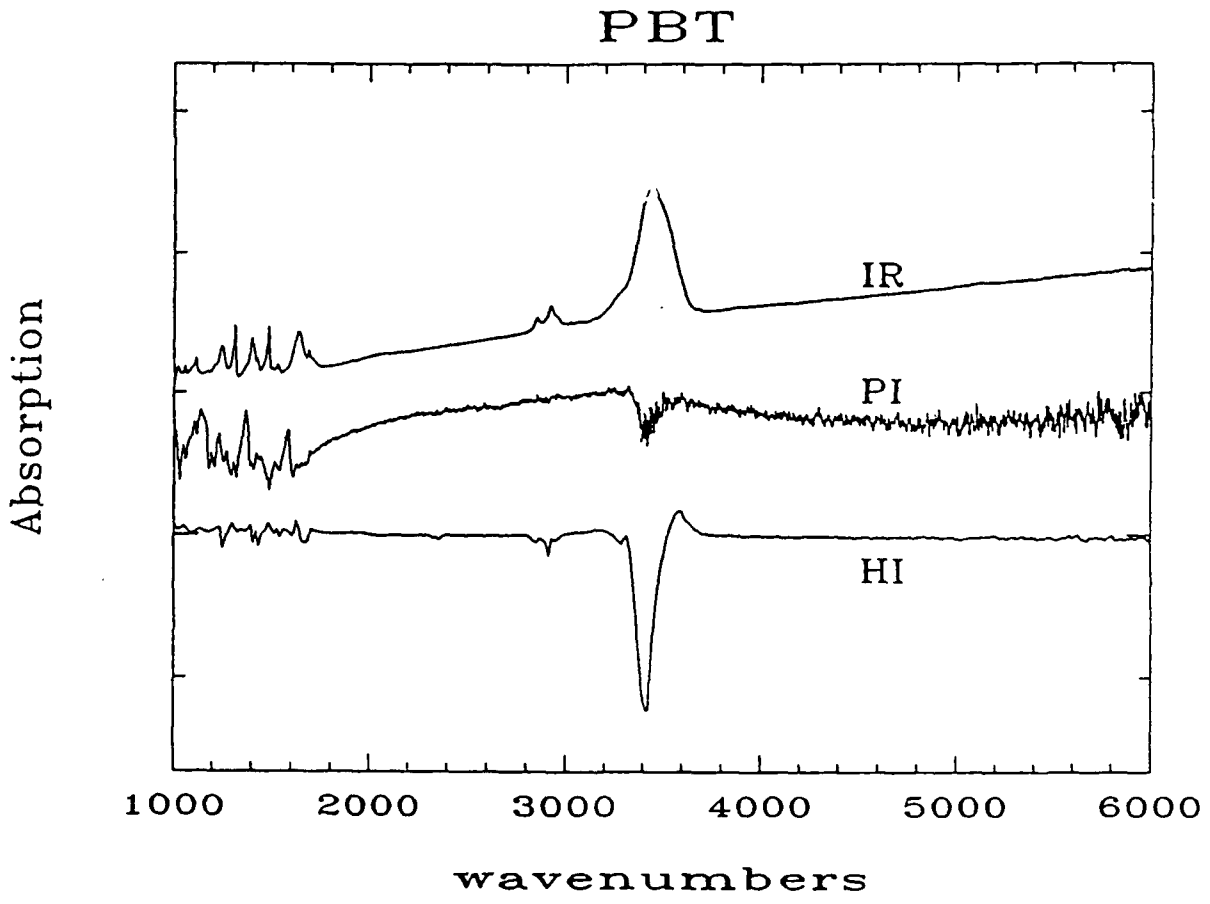

Figure 4a Comparison of direct infrared absorption spectrum, photoinduced absorption spectrum and heating induced effects in PBT.

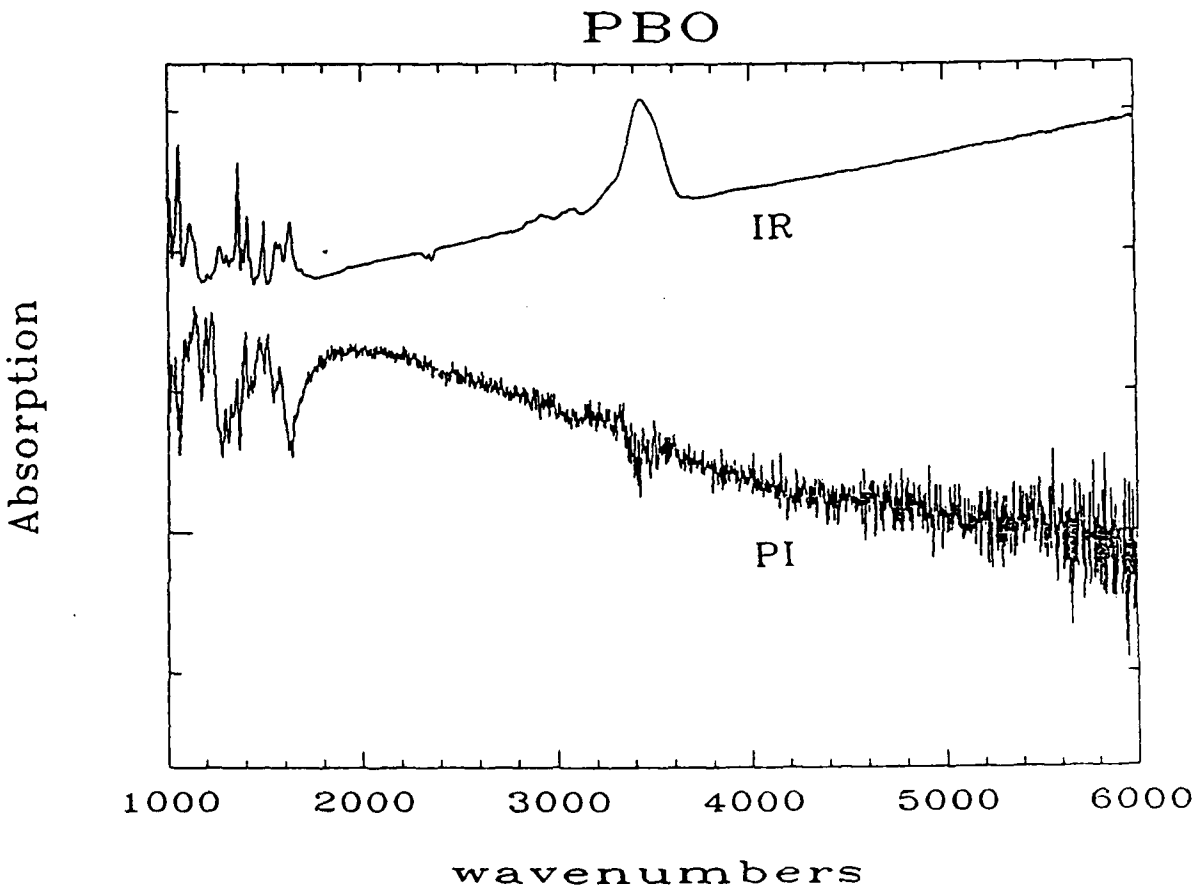

Figure 4b Comparison of the direct infrared absorption spectrum and photoinduced absorption spectrum in PBO.

II.A.ii. Photoluminescence and Electroluminescence Studies of Rigid Rod and Ladder Polymers

Preliminary studies were carried out at The Ohio State University of the photoluminescence of PBO when excited with light of photon energy greater than the band gap energy. Figure 5 compares our photoluminescence spectrum of PBO with the absorption spectrum of PBO. The results support an exciton mediated photoluminescence similar to that of polyphenylenevinylene[18] as well as that reported for BBL.[19] Initial attempts at utilizing an ion implanted region of the polymer as an electrode for a PBO electroluminescence device were unsuccessful.

II.A.iii. Conductivity and Photoconductivity

In conjunction with the postdoctoral researcher working at Wright Patterson Air Force Base, we have studied the unusual thermal and photo conductivity phenomena present in BBL. This is an increase of approximately six orders in conductivity that occurs upon raising the temperature of BBL to 623K and then returning the sample to room temperature (data acquired at WPAFB by Dr. K.S. Narayan). The detailed behavior is dependent upon sample history and moisture content. The slow decay of the increased room temperature conductivity is suggested to arise from the thermal excitation of charge from deep traps. Concomitant EPR studies at OSU of heat treated samples shows a spin concentration that increase with thermal treatment together with a narrowing of the resonance line. While the excess spins decay with time at room temperature, their decay dynamics differs from the decay dynamics of the charge. Further studies are in progress to elucidate the origin of this unusual phenomenon.

Photoconductivity studies were carried out at WPAFB by K.S. Narayan. The action spectrum, Figure 6, shows that the photoconductivity of BBL increases for photon energy greater than the band edge, supporting that the band edge optical absorption is not excitonic. Figure 7 contrasts the temperature dependence of the photoconductivity of BBL recorded for excitation energies below the band gap (8000 Å (1.55 eV)) and above the band gap (6500 Å (1.91 eV)). Total current at photon energies above the gap exhibits an activated behavior with an activation energy total 0.0833 eV. The

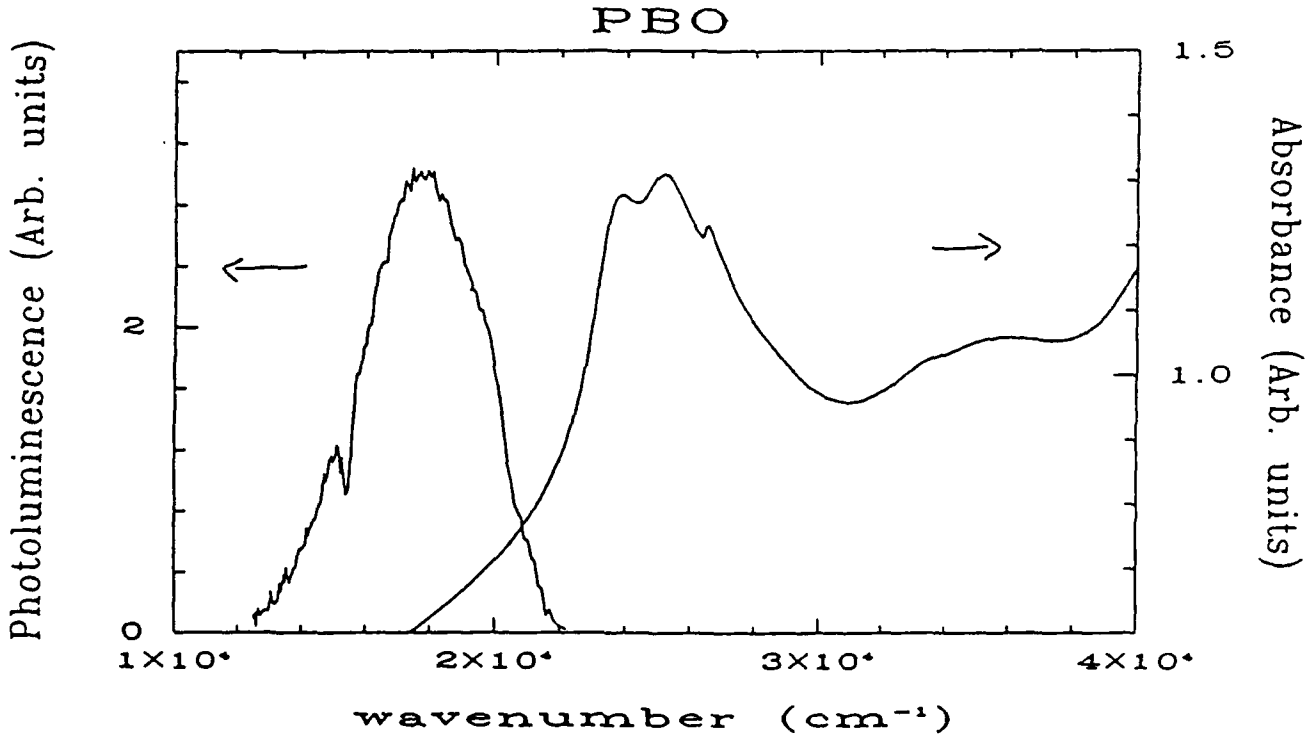

Figure 5 Comparison of photoluminescent and direct absorption spectra of pristine PBO.

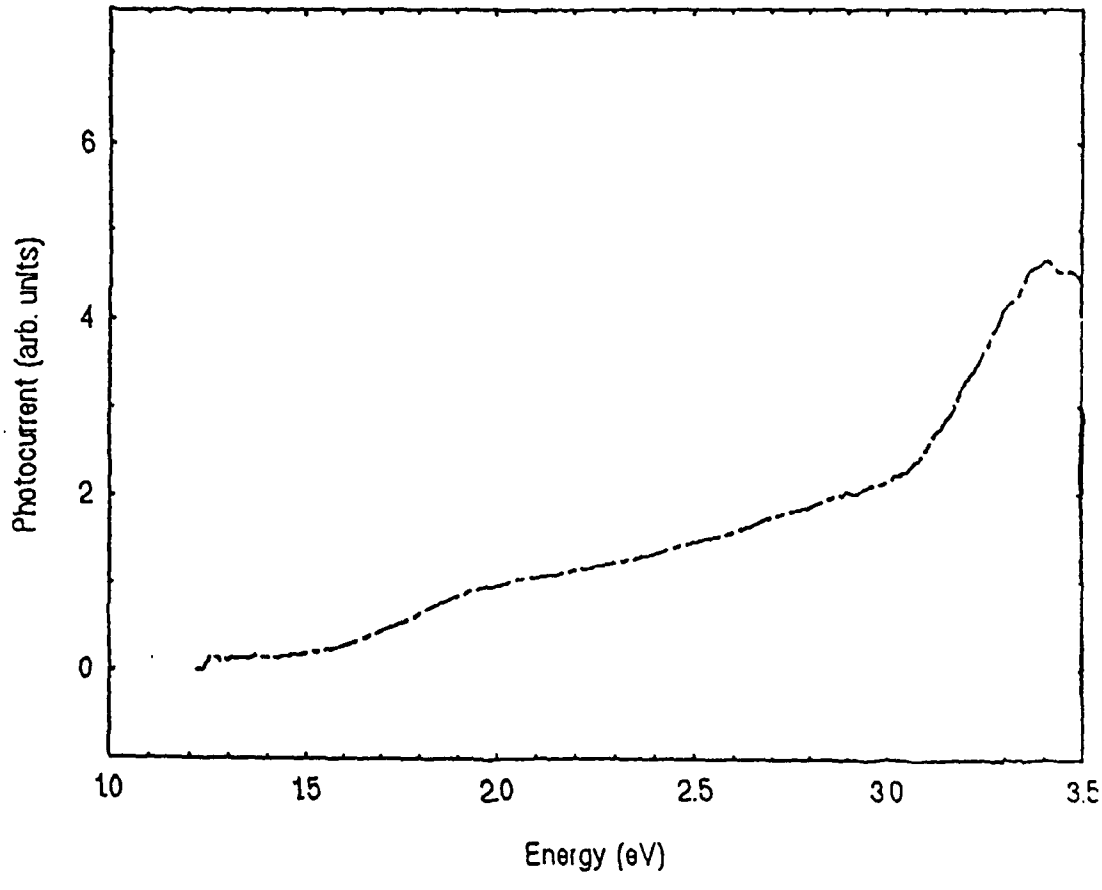

Figure 6 Photocurrent as a function of excitation photon energy in BBL.

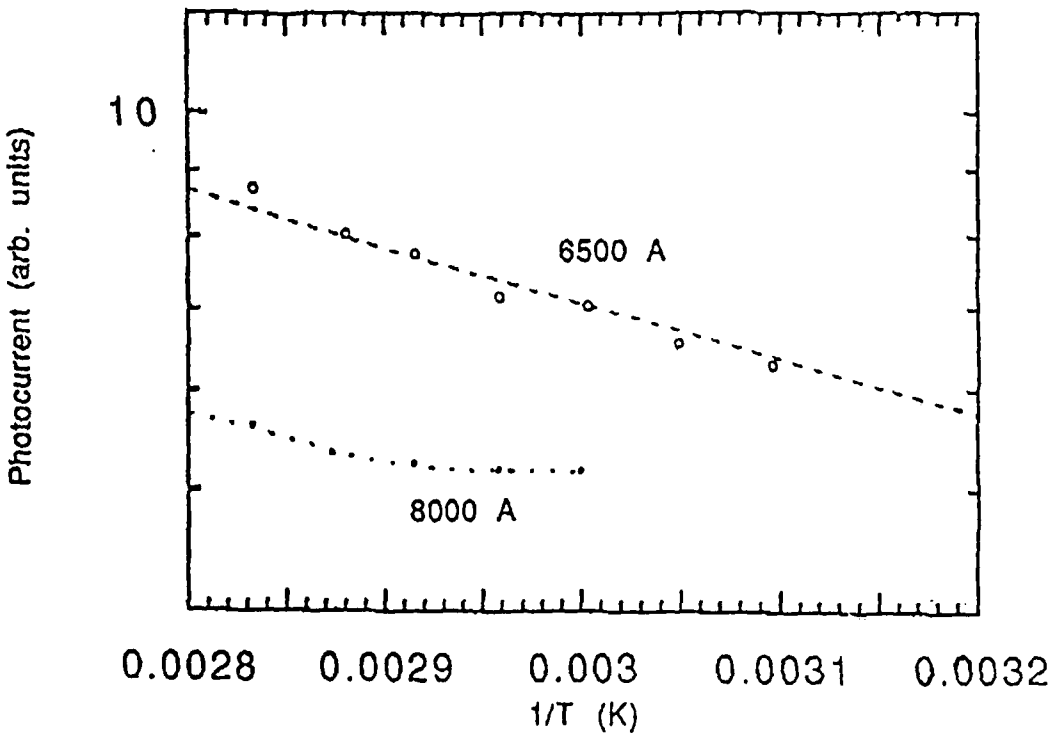

Figure 7 Temperature dependence of the photoconductivity of BBL for excitation energies 1.55 eV (below the band gap) and 1.91 eV (above the band gap).

temperature dependence of the photocurrent for photon energies below the band gap is weaker, without a simple activated behavior. The photoconductivity efficiency is directly related to the product of the charge generation efficiency and the charge mobility. Studies are in progress to further develop a microscopic picture of the control of photoconductivity in these materials.

II.A.iv. Electron Paramagnetic Resonance studies

The room temperature EPR spectrum of the pristine PBO polymer is shown in Figure 8. The ratio $\Delta H_{1/2}/\Delta H_{pp}$ is ~ 1.2 where $\Delta H_{1/2}$ denotes the single integral width of the EPR derivative signal and ΔH_{pp} denotes the peak-to-peak linewidth of the derivative signal. The close agreement with the value expected for a purely Gaussian lineshape, *viz.*, $(2\ln 2)^{1/2} \sim 1.18$, indicates that the spins in the pristine polymer are localized and probably Curie-like. Using DPPH as an intensity standard, the spin susceptibility ($\chi_{pristine}$) at room temperature was determined from the double integral of the EPR derivative signal to be 2.7×10^{-6} emu/mol-repeat. This yields a Curie spin concentration of 2×10^{-3} spins/mole or 1 spin/500 repeat units. From intrinsic viscosity measurements the weight average molecular weight of *cis*-PBO has been estimated at 34,000 which implies ~ 150 repeats/chain. This gives an estimate of 2-3 spins/chain. The origin of these spins needs to ascertained. One possibility is that they are associated with chain ends.

To gain insight into this question, we studied the temperature dependence of the spin susceptibility. Figure 9 depicts the observed behavior in $\chi_{pristine}*T$ as a function of temperature. For non-interacting Curie spins, $\chi*T$ is expected to be a constant, independent of temperature. Instead, the observed decrease in $\chi_{pristine}*T$ upon lowering the temperature suggests an antiferromagnetic coupling between the spins. Assuming a pair-wise interaction within the framework of the Bleaney-Bower model, the data were fit to a sum of coupled and uncoupled spins

$$XT = C + \frac{2N}{3 + \exp(J/T)}$$

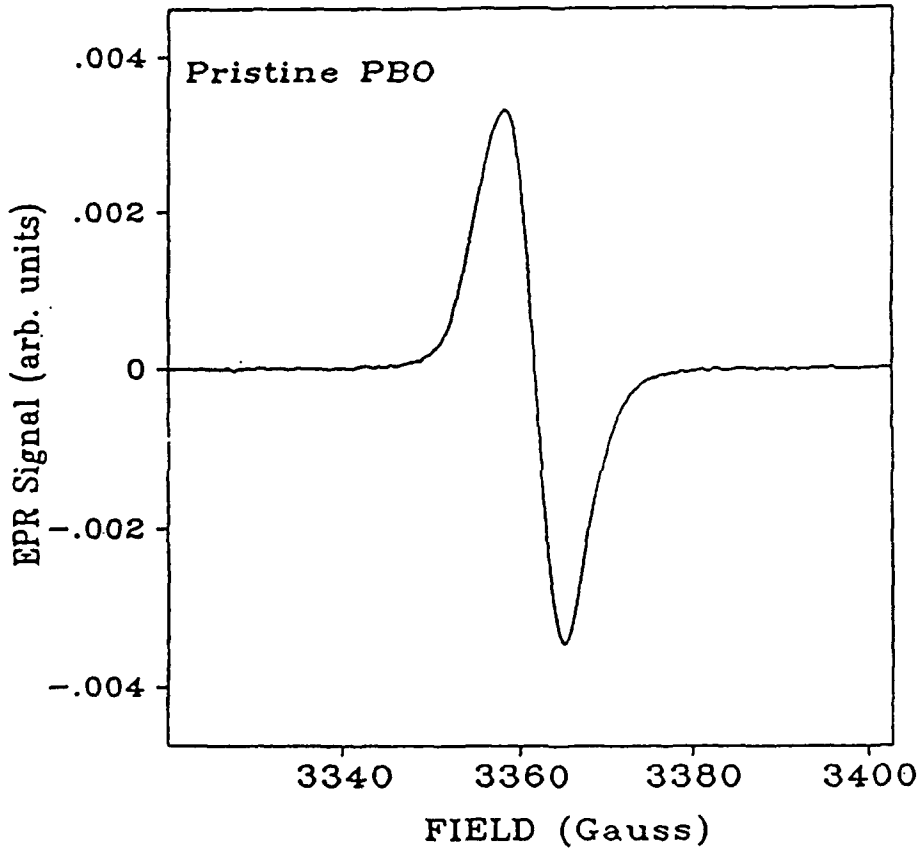

Figure 8 EPR spectrum of pristine PBO at room temperature.

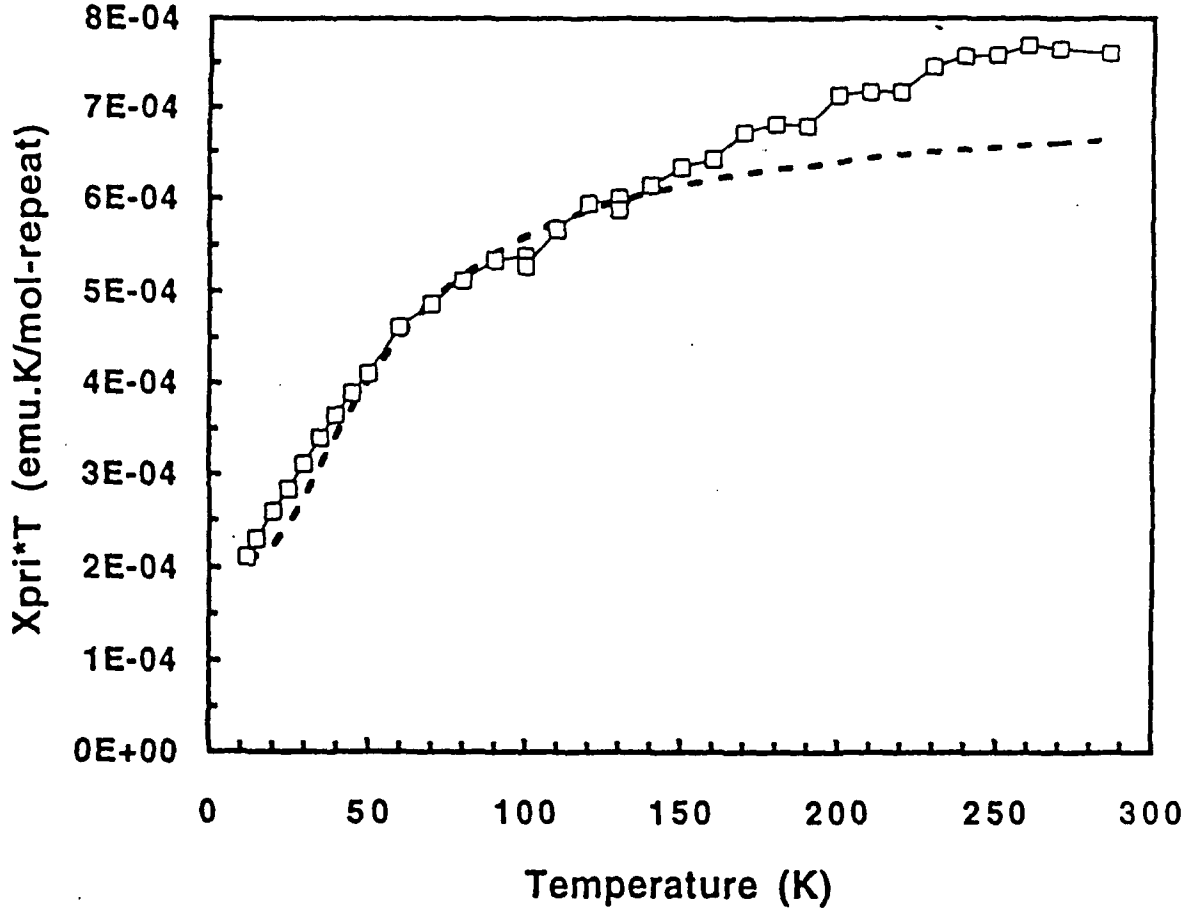

Figure 9 $\chi_{pristine}$*T vs. T of pristine PBO (□). The solid line represents the fit to the data using the Bleaney-Bower equation (see text).

The best fit (see Figure 9) was obtained for an exchange coupling J ~ 100 K and a small number of uncoupled spins, C ~ 0.2(N). As evident from Figure 9, the experimental curve deviates from the fit at high temperatures suggesting a possible distribution in values for the coupling constant J.

II.B. Implanted Rigid Rod and Ladder Polymer Studies

II. B. i. Preparation and Characterization of the Materials

Ion implantation continues to be carried out at Honeywell using samples synthesized at WPAFB and sent to Honeywell through OSU. Studies of PBO, PBT and BBL implanted with $^{84}Kr^{+}$ ions with energies of 200 KeV, were carried out using a current of $2\mu A/cm^2$ and an ion dosage of 4×10^{16} ions/cm^2. We have extended our study to examine the effects of ion implantation dosage selecting biaxial PBO for the study. Samples were implanted with selected dosages in the range of 7×10^{15} to 10^{18} ions/cm^2. Photoemission spectroscopy studies at The Ohio State University show a similar analysis for all systems with higher fluorine content at the lower dosage level, Figure 10(a-c). The likely origin of the impurities is impurities in the glass substrates used for casting films. After ion implantation the oxygen peak is reduced while the carbon peak is relatively enhanced, supporting that the implantation process produces a carbonization of the organic polymer surface.

II. B. ii DC conductivity, thermopower, magnetotransport, and microwave frequency conductivity and dielectric constant studies

The charge transport properties after ion implantation have been studied by Du *et al.*[20,21] Ion implanted PBO, PBT and BBL show essentially indistinguishable charge transport properties. The *T*-dependences of $\sigma(T)$ of these implanted polymers are shown in Figure 11. Above T_C ~ 30K, the data for all samples are fit by $\sigma(T) = \sigma_O + mT^n$ with n = 0.6 - 0.7. A better fit is given by

$$\sigma(T) = \sigma_o + mT^{1/2} + BT. \qquad (1)$$

Equation 1 yields m ≡ 1.3 S/cm$K^{1/2}$, B ≡ 2.8×10^{-2} S/cmK and σ_O ≡ 50 S/cm for all of these implanted rigid rod and ladder polymers regardless of the starting polymers. Below T_C, $\sigma(T)$, decreases more rapidly with *T* and deviates from

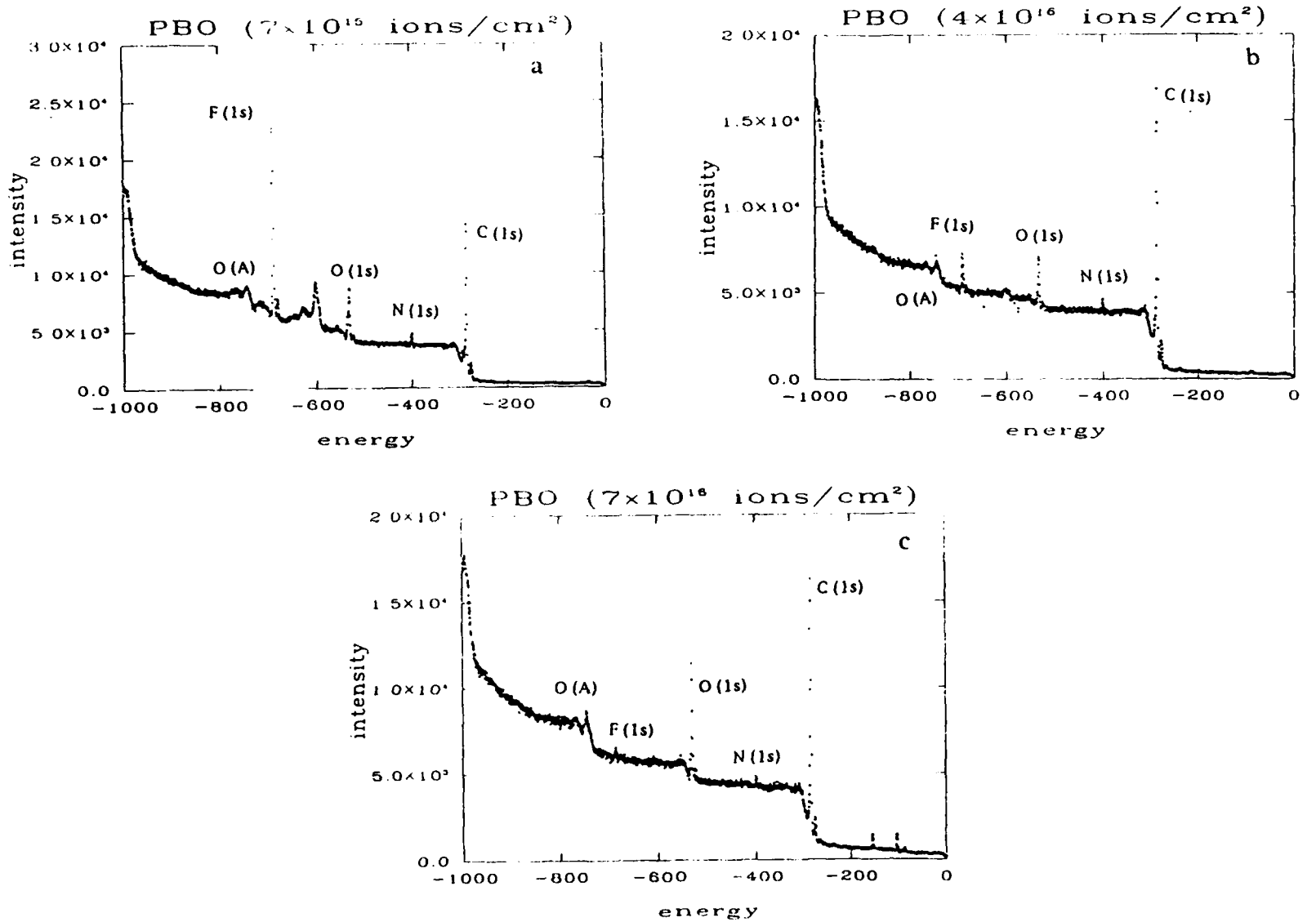

Figure 10 XPS spectra of ion implanted PBO at dosages (a) 7 x 10^{15} ions/cm^2, (b) 4 x 10^{16} ions/cm^2, and (c) 7 x 10^{16} ions/cm^2.

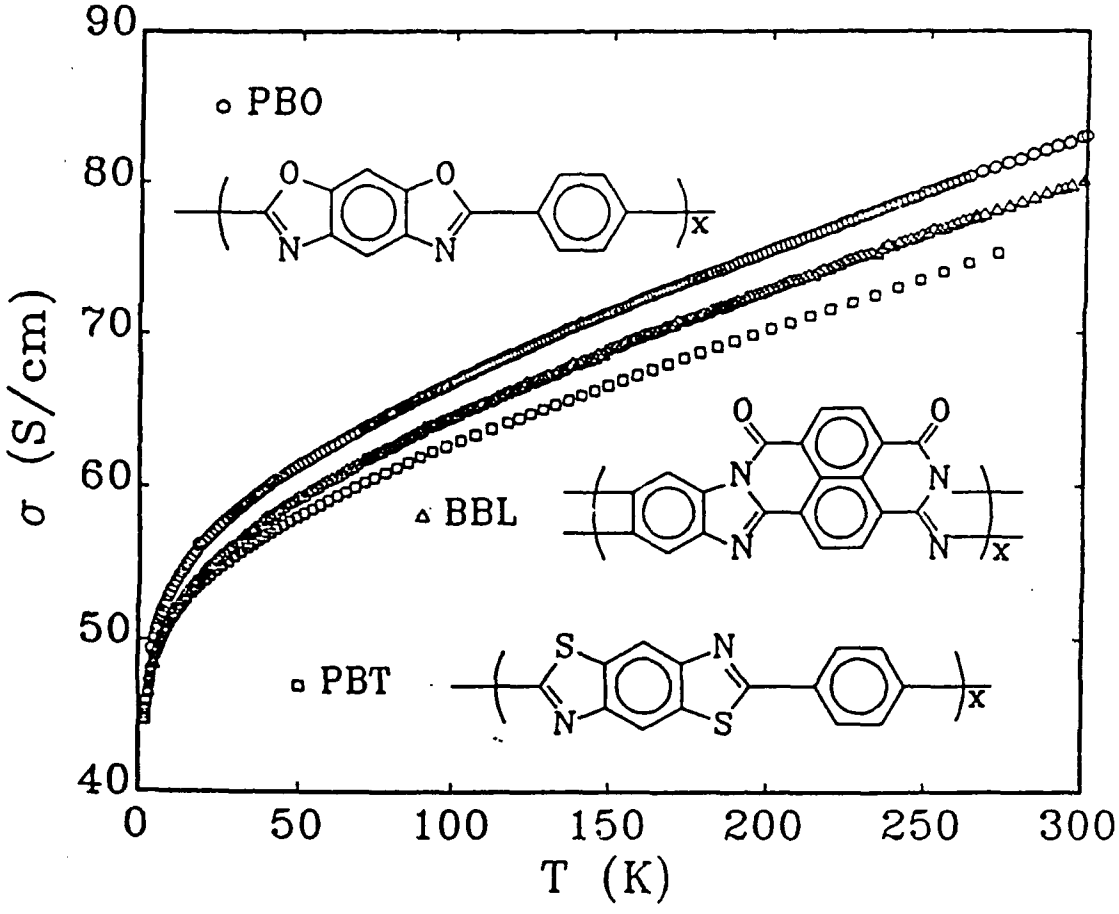

Figure 11 σ(T) vs. T of 4 x 10^{16} ions/cm^2 implanted PBO, PBT, and BBL.

Equation. 1. No other well known models, for example, the variable range hopping conductivity and the activation type conductivity, fit the low temperature range convincingly, which indicates that σ_O is no longer a constant and decreases with T below T_C.

Above T_C, $S(T)$ is small and proportional to T, with a slope of ~ 5.5 x 10^{-3} $\mu V/K^2$, shown in Figure 12. Below T_C, a transition to $S(T) \propto 1/T$ ($S(T)$ increases $T \rightarrow 0$) with a slope of ~ 30 μV for these implanted polymers (see inset, Fig. 12). There is a clear transition from metal like thermopower for $T>T_C$, to a thermopower more typical of a semiconductor with an energy gap at the Fermi energy for $T<T_C$.

All three implanted polymers showed similar magnetoconductance results. A small positive $\Delta\sigma(H,T)$ was observed above T_C and a negative and strongly T- dependent $\Delta\sigma(H,T)$ (which can be fitted to H^2 at low fields and to $H^{1/2}$ at low T and high fields) was observed below T_C. Figure 13 shows the $\Delta\sigma(H,T)$ results of PBO at 4.2 K. Below T_C, a fit of $\Delta\sigma(H.T) \equiv -0.13H/T^{1.5}$ was obtained at low field, and $\Delta\sigma\ (H,T) \propto -1.2H^{1/2}$ was obtained as $T \rightarrow 0$ and at the high field limit (Figure 13, insert).

The spin susceptibility[22] χ of samples implanted with a dosage of 4 x 10^{16} ions/cm^2 have a Pauli term χ^{Pauli} which yields a density of states, $N(E_F)$ ~ 0.1 states/eV-C above T_C (see below). The microwave dielectric constant ε_{mw} (4.2 K) results, obtained from microwave cavity perturbation methods at 6.5 GHz, for all implanted rigid rod and ladder polymers studies for a dosage level of >10^{16} ions/cm^2 are large, ~ 10^4, increasing and remaining positive with increasing T (Figure 14). The large positive ε_{mw} together with its weak temperature dependence for T > 30 K, imply that weak localization is dominant in this temperature regime. Above T_C, ε_{mw} suggests a localization length of approximately 300 Å for these implanted polymers, estimated from $\varepsilon_{mw} \equiv \varepsilon_{-} + e^2\xi^2 N(E_F)$, where ξ is the localization length and ε_{-} is the core dielectric constant. Below 30 K, the strong temperature dependence in ε_{mw} reflects a decrease of the density of states at E_F due to the opening up of a Coulomb gap. There is also a noticeably more rapid decrease in $\varepsilon_{mw}(T)$ below T_C.

Above T_C, the positive $\Delta\sigma(H,T)$ and the T-dependence of $\sigma(T)$ are typical for 3d disordered metals and doped semiconductors for which weak localization

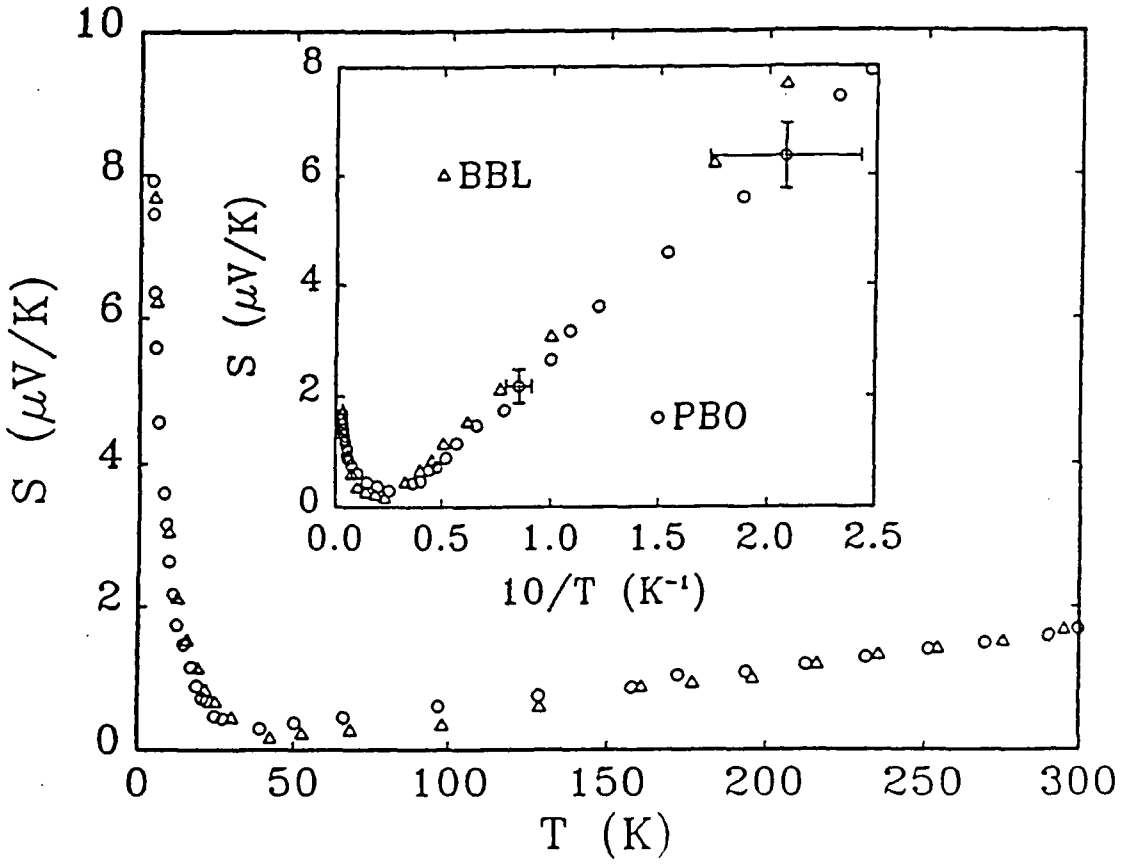

Figure 12 S(T) vs. T of 4 x 10^{16} ions/cm^2 implanted PBO and BBL. Inset: S(T) vs. 1/T of the same data.

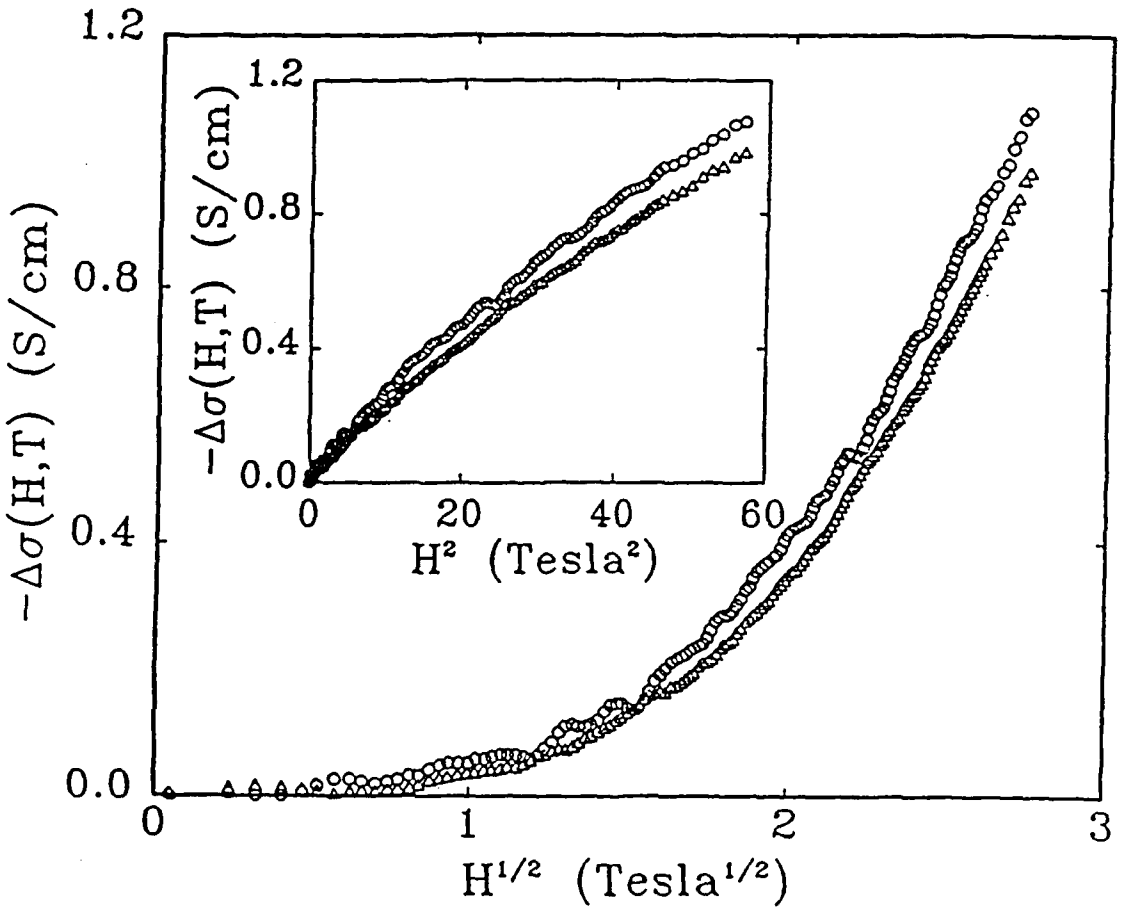

Figure 13 $-\Delta\sigma(H,T)$ vs. $H^{1/2}$ of 4×10^{16} ions/cm^2 implanted PBO at 4.2 K (o for H ∥ I (current) and Δ for H ⊥ I). Inset: $-\Delta\sigma(H,T)$ vs. H^2 of the same data.

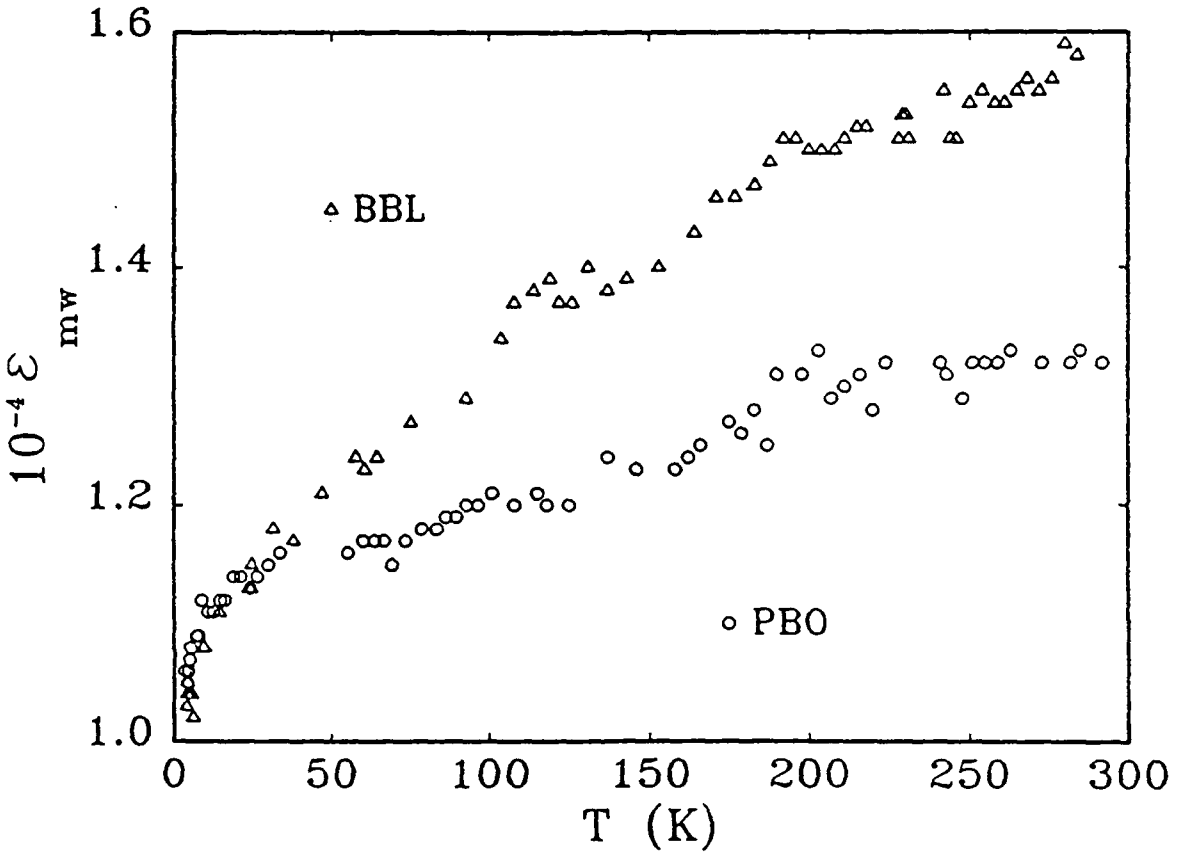

Figure 14 Temperature dependence of the real part of the dielectric constant for 4×10^{16} ions/cm^2 implanted BBL and PBO.

and electron-electron (e-e) interactions dominate the charge transport.[23] Weak localization gives rise to a positive magnetoconductance and e-e interactions are responsible for a negative one,[23]

$$\Delta\sigma_I(H,T) = -\frac{e^2}{4\pi^2\hbar} F\sqrt{\frac{k_B T}{2\hbar D}}\, g_3(h), \qquad (2)$$

where F is the Coulomb screening factor, D is the diffusion constant, $h = g\mu_B H/k_B T$, $g \equiv 2$ is the Landé factor measured by EPR, $g_3(h) \equiv 0.053\eta^3$ for $H \ll 1$, and $g_3(h) \equiv \sqrt{h} - 1.3$ for $h \gg 1$. The small positive $\Delta\sigma(H.T)$ shown in the $\Delta\sigma(H,T)$ data above T_C (Figure 15) is presumably the net result of the addition of the two effects with weak localization dominating e-e- interactions. Below T_C, the negative and strongly T-dependent magnetoconductance results suggest that the weak localization term disappears because it has the opposite sign and a stronger temperature dependence than the e-e interaction term (Eqn.) 2. The magnetoconductance results would be positive below T_C if the weak localization term persisted. At low field ($h \ll 1$) Eqn. 2 yields $\Delta\sigma_I(H,T) \equiv -0.151(F/\sqrt{D})(H^2/T^{3/2})$; comparing to Fig. 15, $F/\sqrt{D} \sim 0.66$ is obtained, in good agreement with the low field result. Thus, the fit of $\Delta\sigma$(H,T) data below T_C to Eqn. 2 supports that e-e interactions totally dominate the transport at low temperatures.

The weak localization effect also predicts a correction term to the dc conductivity for the 3d case: $\Delta\sigma_L(T) = (e^2/2\pi^2)(T_{tiv})1^{/2}$, where $T_{in} \propto T^{-P}$ is the inelastic scattering time, with $p = 2$ for clean metals and $p = 3/2$ for dirty metals.[22-24] Thus, $\Delta\sigma_L \propto T$ in the clean limit and $T^{3/4}$ for the dirty limit. While the e-e interaction effect provides a correction term in the 3d case.[23-25]

$$\Delta\sigma_I(T) = \frac{e^2}{4\pi^{2\hbar}} \frac{1.3}{\sqrt{2}} \left(\frac{4}{3} - \frac{3}{2}F\right)\sqrt{\frac{k_B T}{\hbar D}}. \qquad (3)$$

Thus, the applicability of Eqn.. 1 to $\sigma(T)$ $T > T_C$ suggest that both weak localization and e-e interaction effects contribute to the conductivity in this regime. Utilizing Eqn. 3 and taking the fitting result from Eqn. 2 $F/\sqrt{D} \equiv 0.76$, $D \sim 4.3$ cm^2/sec is obtained from the coefficient $m = 1.3$. S/cmK$^{1/2}$ of the $T^{1/2/}$ term Eqn. 1. Using this D and comparing the predicted $\Delta\sigma$(T) with the linear T term of Eqn. 1, $\tau_{in} = 4.5x10^{-8}T^{-2}$ sec is then obtained.

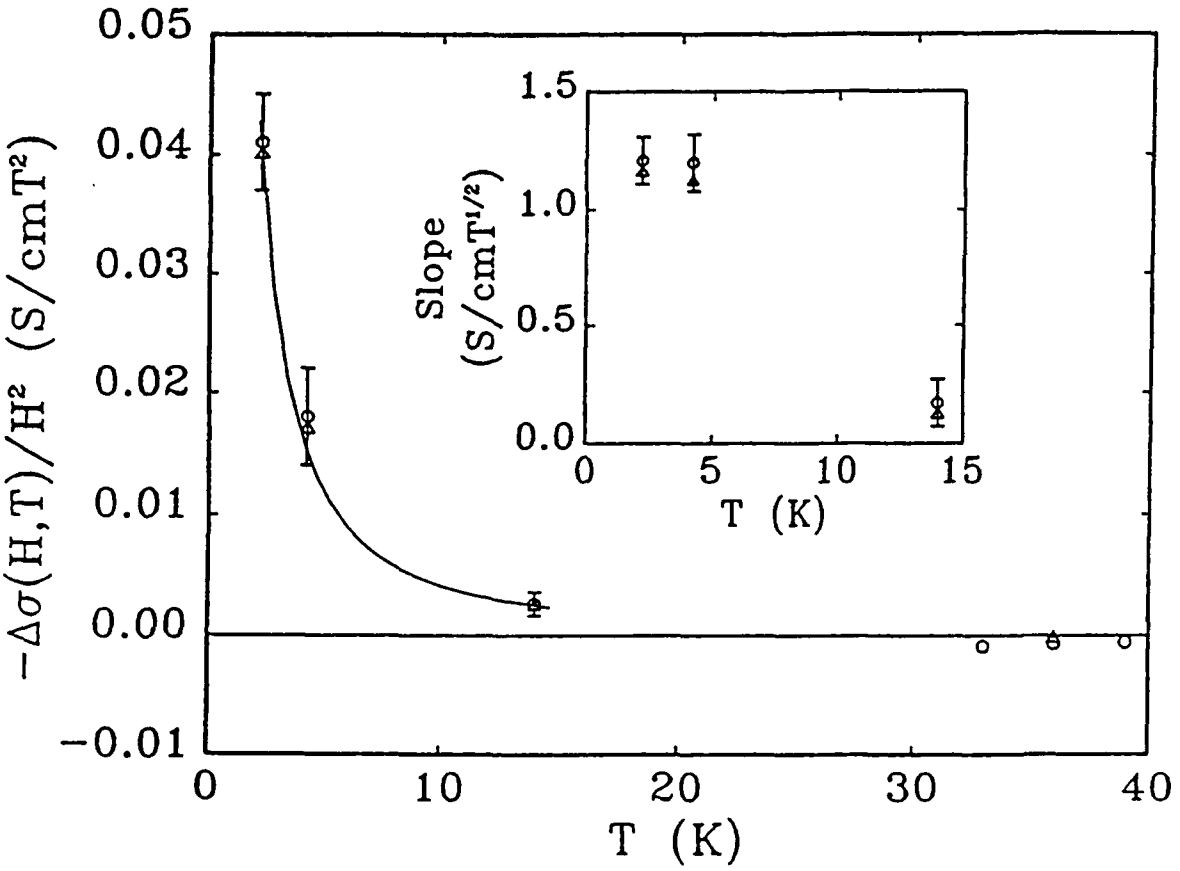

Figure 15 $-\Delta\sigma(H,T)/H^2$ (the slope of the data curve of Figure 13 inset as $H \rightarrow 0$) vs. T for 4×10^{16} ions/cm^2 implanted PBO (o) and BBL (Δ). The solid line is a fit of $-0.13/T^{3/2}$. Inset: the slope of the asymptote of $-\Delta\sigma(H,T)$ (Figure 13) at the high field limit vs. T. The slope $\rightarrow$ 1.2 S/cm $T^{1/2}$ as $T \rightarrow 0$.

The characteristic length[24] $(\hbar D/k_BT)^{1/2}$ is then calculated at 30 K to be 110 Å, much smaller than the sample thickness (~ 3500 Å). This is self-consistent with the application of the 3d model. Also, a small screening factor F ~ 1.6×10^{-2} is obtained. The small DOS (from χ^{Pauli}), the large localization length ξ (from $\varepsilon_{\mu\omega}$), and the featureless broad band absorption[25] are also consistent with this semi-metallic picture. Based on this model, the small and linearly *T*-dependent *S(T)* can be understood to be due to the small semi-metallic DOS.

Below T_C, the change of sign in the $\Delta\sigma$ *(H,T)* behavior shows that e-e interactions become more important and eventually dominate the charge transport.[23,24] The more rapid dropping of σ_0 and $\varepsilon_{mw}(T)$ (Figures 11 and 14) with *T* indicates a decrease in the DOS at the Fermi Level (recall the Einstein relation[25] $\sigma_O = e^2DN(E_F)$, and $\varepsilon_{mw} \cong \varepsilon_\infty + e^2\zeta^2N(E_F)$). These results, together, indicate the opening of a Coulomb gap below T_C. As T is lowered, electron localization may increase, and such an increase, in turn, reduces electron screening and enhances e-e interactions. The proposed depletion of the DOS at the Fermi energy may suppress the quantum interference effect and account for the disappearance of the weak localization correction term in the magnetoconductance results. Though σ(T) decreases more rapidly below T_C, it remains semi-metallic at 0.1 K (σ(0.1 K) ≅ 30 S/cm) which suggests that the DOS is probably zero only at E_F, in accord with the theoretical predictions of the 'Coulomb' gap.[23] The semiconductive 1/T-dependent S(T) at low T and the large ε_{mw} (typical for a semiconductor with a small gap are also in accord with the assumption of a Coulomb gap. However, this low temperature regime is not a 'simple' insulating regime, as the conductivity results follow neither the variable range hopping model nor an activation type conduction, and the conductivity and the dielectric constant are still large.

The origin of the semi-metallic phase of implanted PBO, PBT, and BBL, the low T energy gap, and the difference in their behavior from earlier studied implanted polymers (for example, implanted polyparaphenylene sulfide, which showed strongly localized behavior[13,14]) is of particular interest. The earlier studied implanted polymers do not have the spatial relationships for carbon atoms as present in PBO, PBT, and BBL. Hence, we propose that upon impact by energetic and massive ions, and the subsequent breaking of bonds (and evolution of non-carbon atoms,[26,27] the re-formed carbon network forms a 3d interconnected graphite-like network for

implanted ladder and rigid rod polymers. This assertion is supported by X-ray photoemission spectroscopy studies which show the implanted surface is almost entirely carbon (Figures 2 and 10), and the preliminary Raman spectra studies which show graphite-like bonding among carbons after ion implantation.

When the thermal energy k_BT is comparable or smaller that the Coulomb interactions (below T_C), the Coulomb gap is likely to be evident. It is unlikely that this transition is introduced by other structural changes, for example, a Peierls transition, as these implanted polymers are amorphous and three dimensional. A dimensional cross-over is not the cause of this transition either, since the characteristic length $(\hbar D/k_BT)^{1/2}$ at 1 K would be ~600 Å, still smaller than the samples thickness (~ 3500 Å). An initial estimation of the size of the 'Coulomb' gap can be obtained by using the semiconductive dielectric constant $\varepsilon = 1 + (\hbar\omega_p/E_g)^2$ where $\omega^2 p = 4\pi ne^2/m$. We thus obtain E_g ~ 2 meV. This value is in a good agreement with T_C (~ 2.6 meV).

In summary, the charge transport properties of ion-implanted rigid rod and ladder polymers *differ substantially from* those of previously studied implanted polymers. An unusual metal-nonmetal transition exists at a finite temperature which is interpreted in term of a Coulomb gap opening up in the semi-metallic regime.

II. B. iii EPR Spin Susceptibility Studies

A typical room temperature EPR spectrum of a PBO sample, implanted at a fluence of 4×10^{16} is shown[23] in Figure 16. It consists of contributions from spin susceptibilities of the implanted as well as pristine layers. Though the thickness of the implanted layer is less than 2% of the total thickness, the two contributions were successfully resolved. It was found that at room temperature, the double integral (DI) of the EPR derivative signal contains nearly equal contributions from the two sets of spin susceptibilities, implanted and pristine. At low temperatures, $(DI)_{implanted}$ is a factor of 3 larger than $(DI)_{pristine}$, further improving the accuracy with which the spin susceptibility of the implanted polymer, $\chi_{implanted}$, could be obtained.

Figure 17 shows a plot of $\chi_{implanted}$*T as a function of temperature. There is an unusual temperature dependence in the observed behavior;

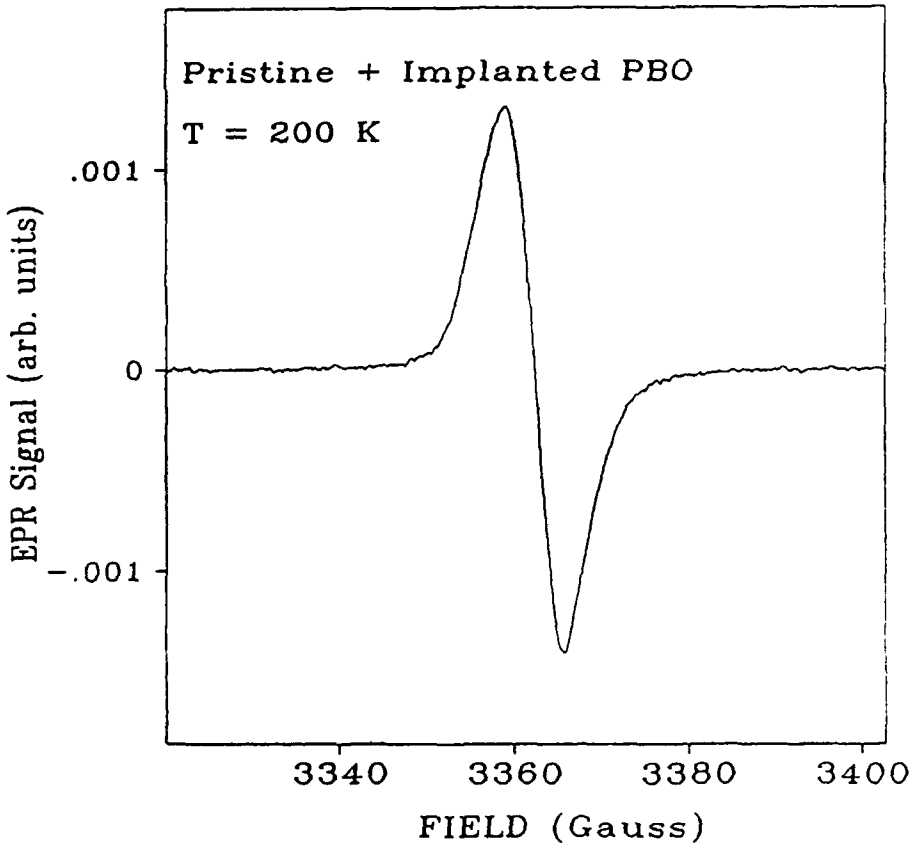

Figure 16 Room temperature EPR spectrum of PBO implanted at a fluence of 4×10^{16} Kr^{+} ions/cm^2.

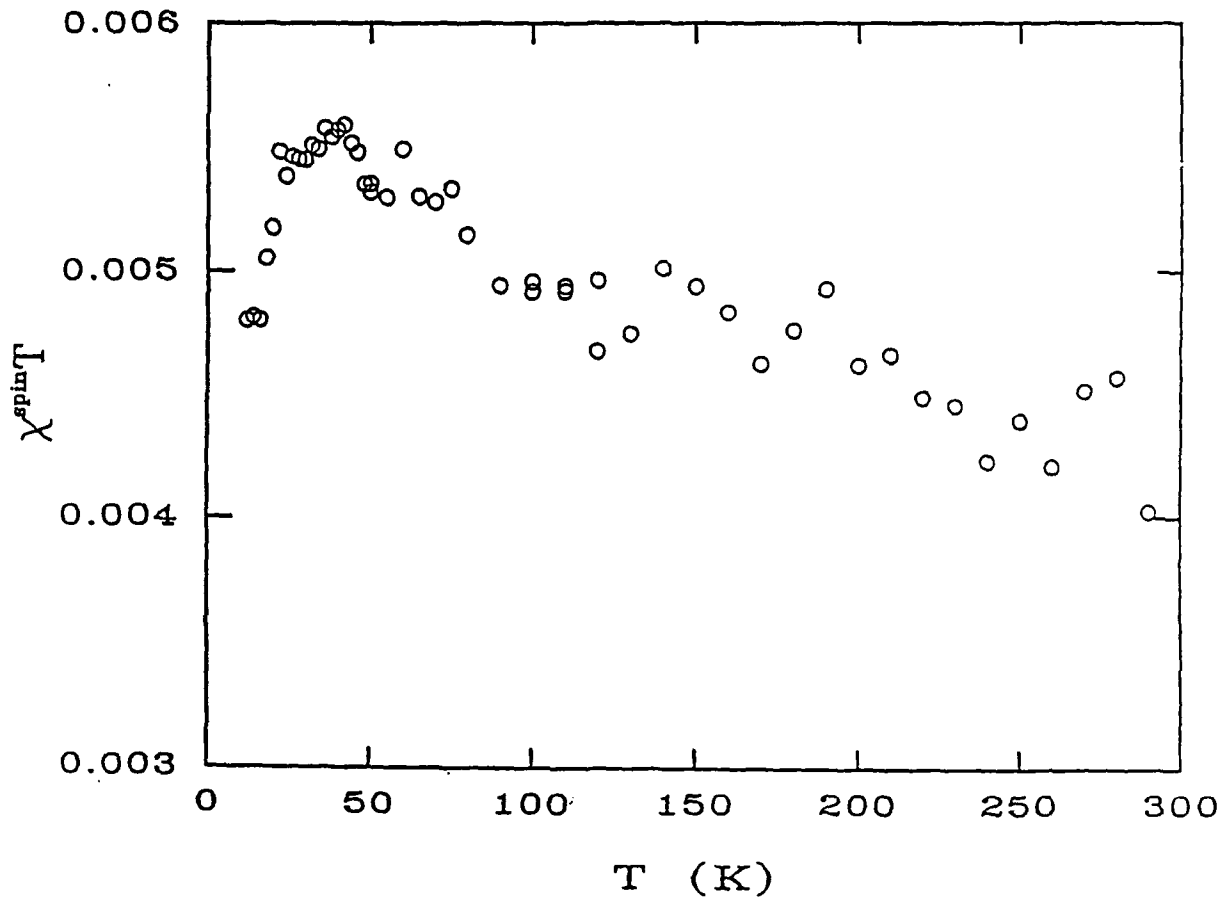

Figure 17 $\chi_{implanted} * T$ vs. T for 4×10^{16} ions/cm^2 implanted PBO.

$\chi_{implanted}$*T increases upon lowering the temperature, reaches a maximum at T ~ 30 K, and then shows a steep decrease for T < 30 K. The trend indicates that the material undergoes a transition at T_C ~ 30 K. This is in remarkably good agreement with the conclusion reached from the OSU charge transport studies that an anomalous metal to non-metal transition occurs at ~ 30 K, with a collapse in the density of states at E_F [$N(E_F)$] for T < 30 K. Such a suppression in the $N(E_F)$ is expected to result in a decrease in χ*T, consistent with the observed behavior (see Figure 17).

For the $T > T_C$ regime, the unusual increase in $\chi_{implanted}$*T with decreasing T has been examined within the context of several models. It is recalled that in this temperature regime, the material is postulated to be semi-metallic with weak localization. Here U denote the effective Coulomb repulsion between electrons. In model 1, we consider, in addition to the usual Curie and Stoner terms, the contribution to the susceptibility from the diffusive motion of spin fluctuations:[23]

$$\Delta X \sim -\left[\frac{\mu_B^2 U N(E_F)^2}{(k_F l)^{3/2}(E_F)^{1/2}}\right] T^{1/2} = -AT^{1/2}$$

$$\Rightarrow XT = -AT^{3/2} + X_S^{Pauli} T + b^{Curie}$$

Using typical values for the parameters U, $N(E_F)$, k_F, and l, the estimated value of $\Delta\chi$ is six orders of magnitude smaller than χ^{Pauli}. Thus, model 1 fails to explain the observed enhancement in $\chi_{implanted}$*T with decreasing temperature.

Model 2 makes the *ansatz* that $N(E_F)$ is temperature dependent and increasing for the T > 30 K regime. This could in principle explain the observed trend in $\chi_{implanted}$*T. However, the thermoelectric power which is a sensitive probe of $N(E_F)$ because

$$S(T) \propto \frac{1}{N(E_F)} \frac{d[N(E_F)]}{dE} T,$$

shows a linear temperature dependence in this regime. This implies that $N(E_F)$ ~ constant for T > 30 K, eliminating model 2.

In model 3, the spin susceptibility of the implanted polymer is decomposed into Pauli and Curie components,

$$X_{Im\,planted}^{Pauli} = \frac{\mu_B^2 N(E_F)}{1 - U(T) N(E_F)}$$

and $X^{Curie}_{Implanted} = \frac{b(T)}{T}$.

There are two limiting cases to this model. In one limit, the Curie constant 'b,' and hence the Curie spin concentration N^{Curie} is assumed to be independent of temperature. The enhancement in $\chi_{implanted}*T$ is totally attributed to a temperature dependent Coulomb repulsion U(T). If we assume that at room temperature U=0; then upon lowering the temperature, we conclude that there is a decrease in the localization length intuitively suggesting an increase in the effective electron repulsion. From optical results on implanted PBO (see Figure 3), it is evident that the bandwidth of the material is greater than 6 eV, whereas π-conjugated carbon systems have a bandwidth of ~ 10 eV. Selecting an intermediate value of 8 eV for the bandwidth implies an $N(E_F) \sim 0.125$ states/eV-C. This yields a rather strong temperature dependence in U as depicted in Figure 18.

In the other extreme limit of this model, $X^{Pauli}_{Implanted}$ is assumed to be constant, independent of temperature. The observed enhancement in $\chi implanted*T$ is entirely attributed to a temperature dependent N^{Curie}. The resulting variation in N^{Curie} with temperature for T > 30 K is shown in Figure 19. The behavior is suggestive of thermal deactivation of itinerant spins to localized spin states.

II. B. iv Implantation Dosage Dependent Insulator to Metal Transition

Figure 20 is a plot of the conductivity of samples normalized to that for the sample subject to a flux of 10^{18} ions/cm^2 as a function of ion dosage ϕ on a double logarithmic scale. It is assumed that the thickness of the implanted layer is the same for each of these samples. It can be seen that a dosage dependent insulator to metal transition occurs at $\phi \sim 4 \times 10^{16}$ ions/cm^2. Saturation of the conductivity occurs at $\phi \sim 10^{17}$ions/cm^2.

The charge transport in lower dosage samples is more strongly temperature dependent than that of the heavily implanted discussed above. Figure 21 shows that the room temperature conductivity for the sample with a dosage of 7×10^{15}ions/cm^2 is about 10^{-1} S/cm similar to that of earlier study of implanted materials. Most of the implanted materials of such a low dosage have a conductivity which is proportional to $\exp(-(T_O/T)^{1/2})$ for a large

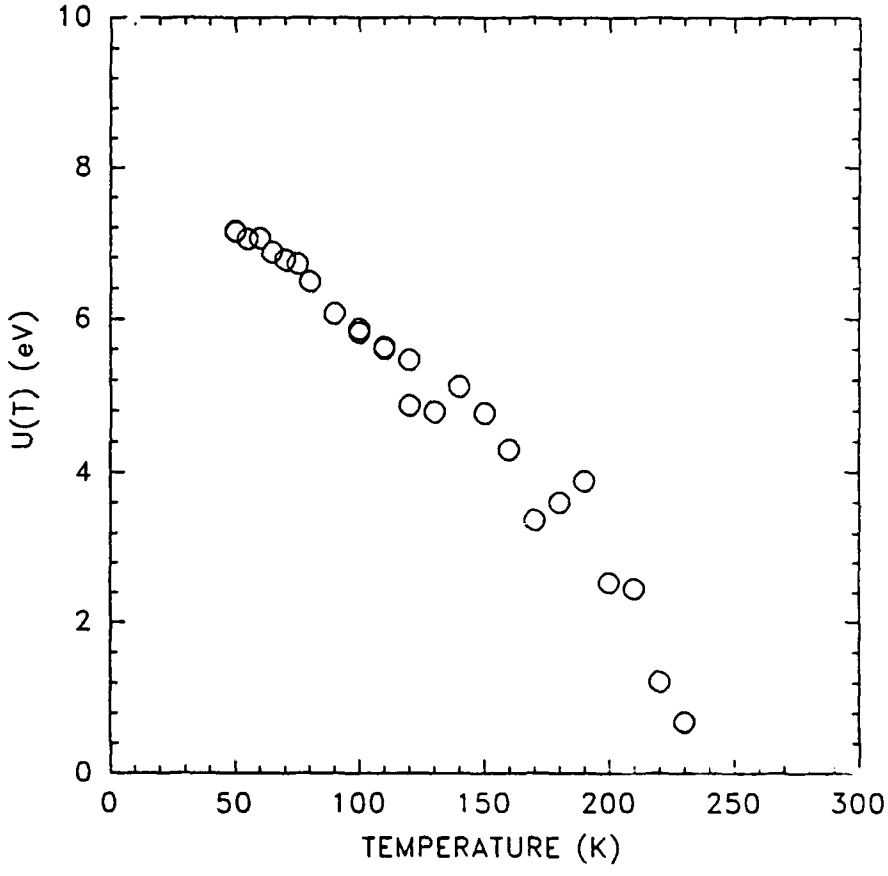

Figure 18 Estimated temperature dependence of the effective Coulomb repulsion (U) in 4×10^{16} ions/cm^2 implanted PBO (see text); Data is from Figure 17.

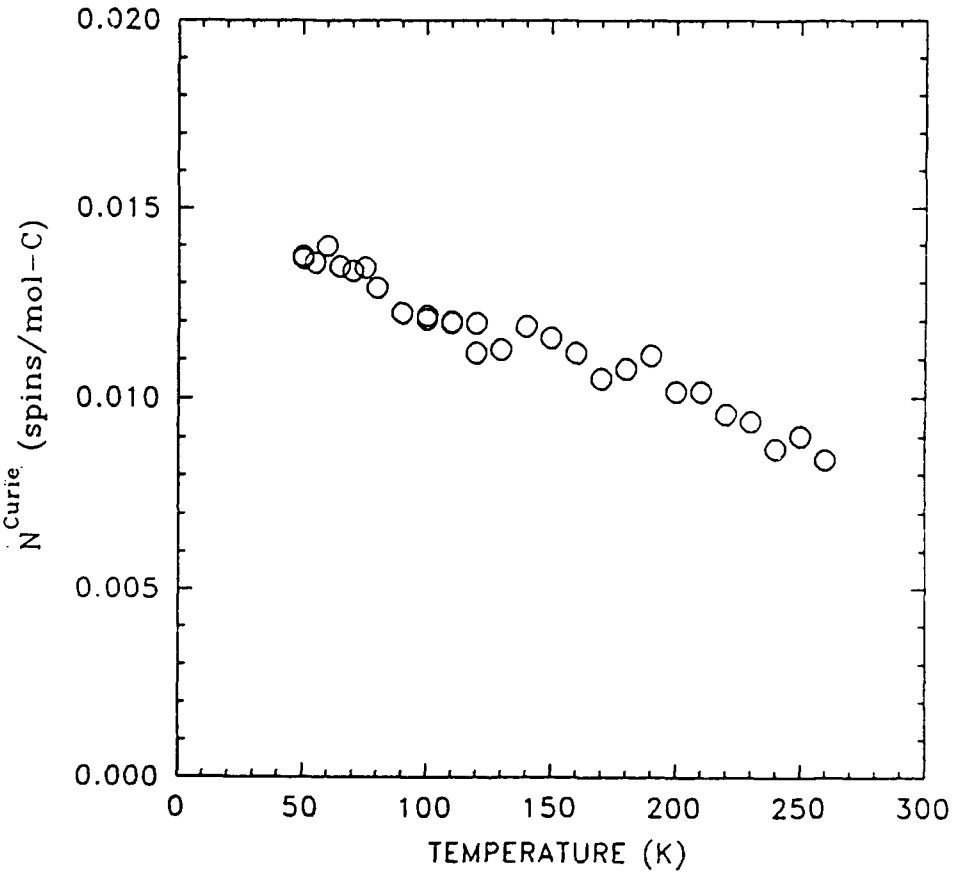

Figure 19 Temperature dependence of the effective Curie spin concentration for 4×10^{16} ions/cm^2 implanted PBO (see text); Data is from Figure 17.

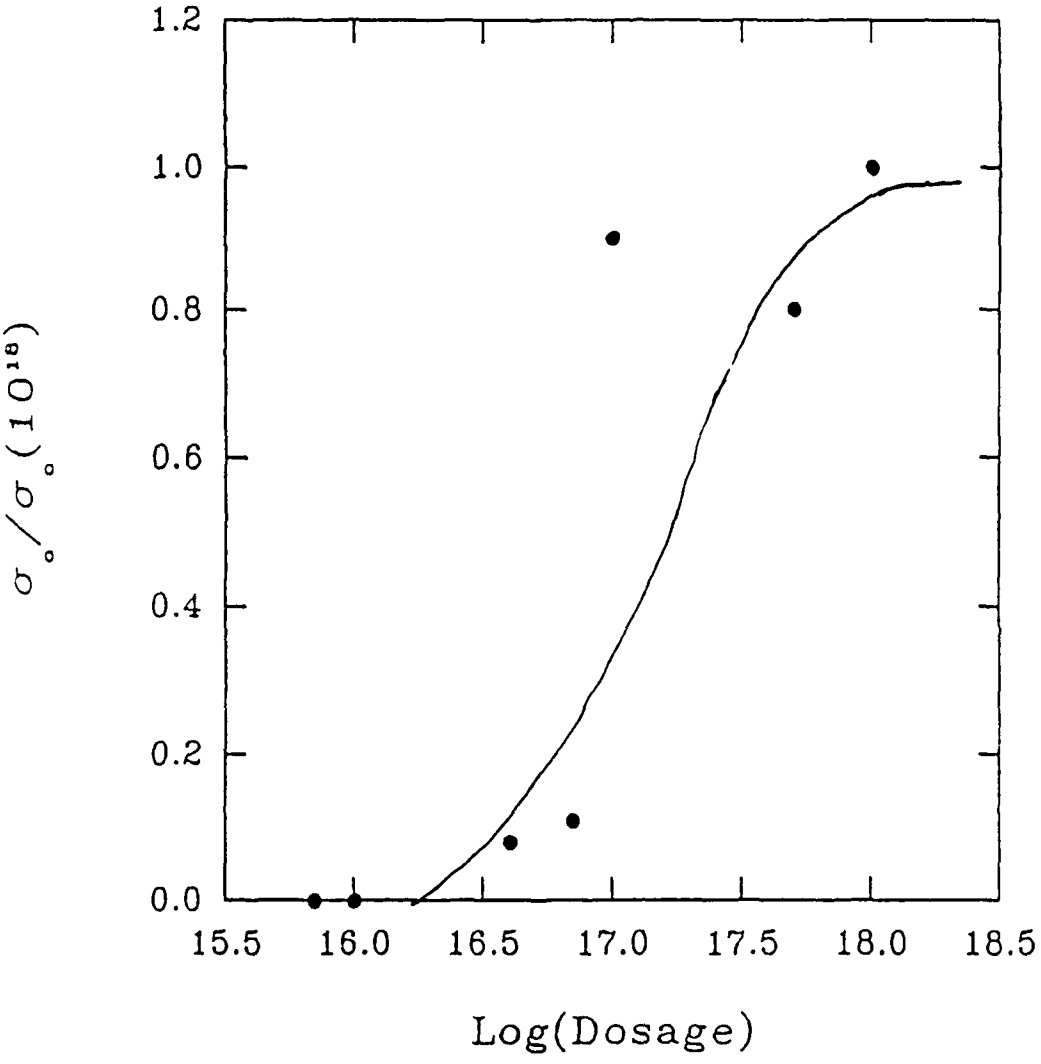

Figure 20 Log($\sigma_O/\sigma_O(\phi \approx 10^{18})$) vs. Log($\phi$) of implanted PBO.

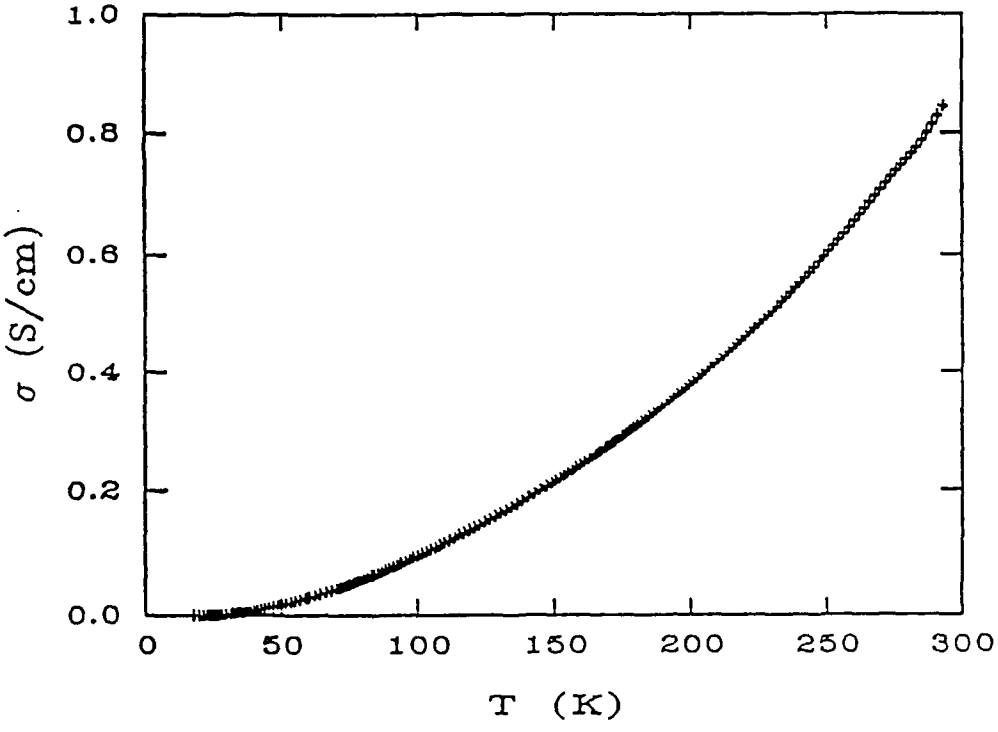

Figure 21 DC conductivity vs. T of implanted PBO with $\phi = 7 \times 10^{15}$ ions/cm^2.

temperature range. Figure 22 shows the log of dc conductivity versus $T^{-1/2}$, as well as vs. T^{-1} and $T^{-1/4}$ for the PBO sample exposed to a dosage equal to $\phi = 7 \times 10^{15} cm^{-2}$. From the data it is clear that the temperature dependence of conductivity changes with temperature. The dielectric constant measured at microwave frequency for the lower dosage sample is contrasted with that of the higher dosage sample in Figure 23. The observed microwave frequency dielectric constant of the low dosage sample is about two orders of magnitude smaller than that of the 'metallic' samples and is almost temperature independent. Assuming the same density of states at the Fermi level as the higher dosage sample, we estimate a localization length of a total of 20Å for the low dosage sample. This is much smaller than the 500Å localization length estimated for the higher dosage sample.

The insulator to metal transition that occurs as a function of increasing ion dosage is attributed to an Anderson transition. This transition arises from the reorganization of electronic structure caused by implantation process. Within this model, with increasing ion dosage the Fermi level is moved past the mobility edge causing the Anderson transition.

II. B. v Thermal Cycling Stability

Table 1 shows the University of Rochester measured room temperature conductivity of the annealed sample (σ_a) normalized with the conductivity of the unannealed sample (σ_{ua}). The measured conductivities of the heat treated implanted samples were found to be essentially the same as the unannealed samples over the entire range of annealing temperatures, 50-400°C as exemplified in Figure 24 for the conductivity of implanted PBO. The slight variations are within experimental errors. This observation is in sharp contrast to the reported[29] heat treated implanted DPBI, DPBO, DPBT and BBL that showed approximately three orders of magnitude decrease in the conductivity after annealing at 400°C for 40 mins. It must be emphasized, however, that the implantation conditions used in the latter (190 keV, 0.1 $\mu A/cm^2$ beam current) are different from the ones used here which might influence the nature of the interactions of the Kr^+ ions with the substrate. The beam intensity used here is a factor of 20 greater than the ones used in earlier studies,[29] which might be the reason for the ready release of the Kr^+ ions when annealed at high temperatures. The conditions used in this study

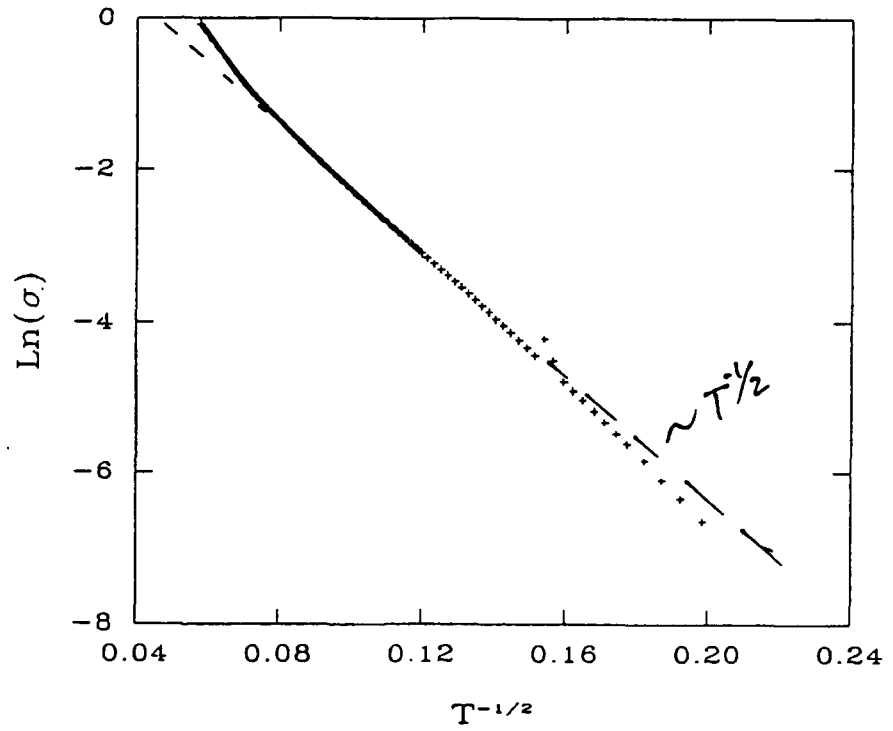

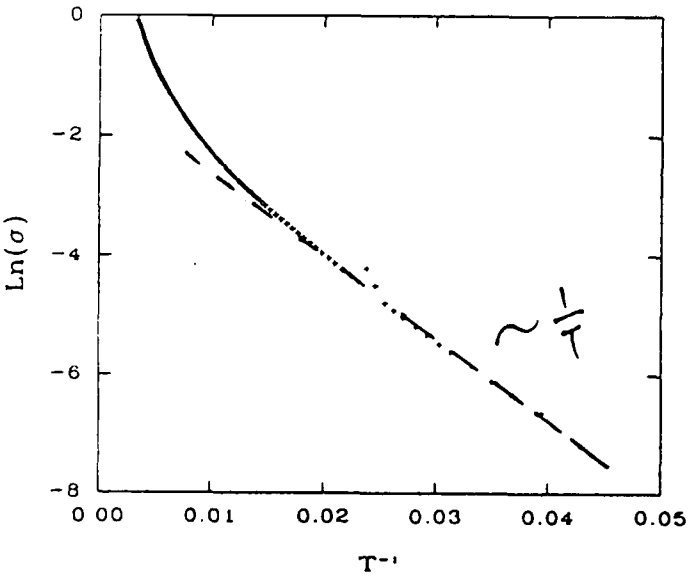

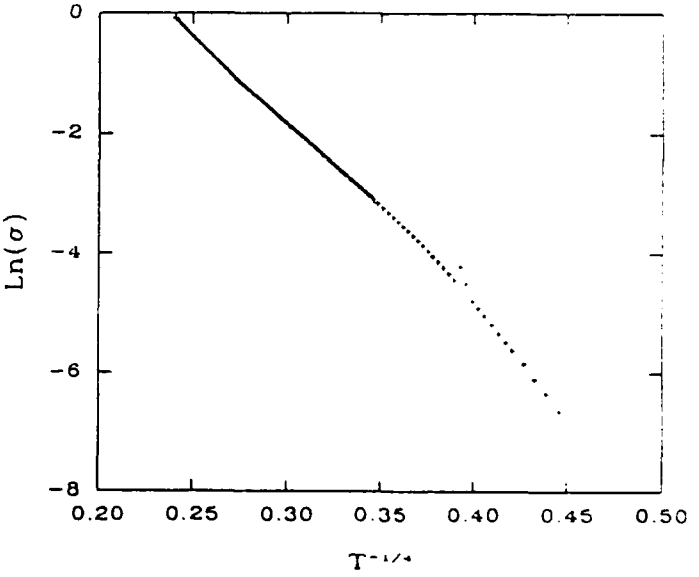

Figure 22 DC conductivity fittings of the low dosage implanted PBO sample: (a) Ln(σ) vs. $1/T^{1/2}$, (b) Ln(σ) vs. 1/T, and (c) Ln(σ) vs. $1/T^{1/4}$.

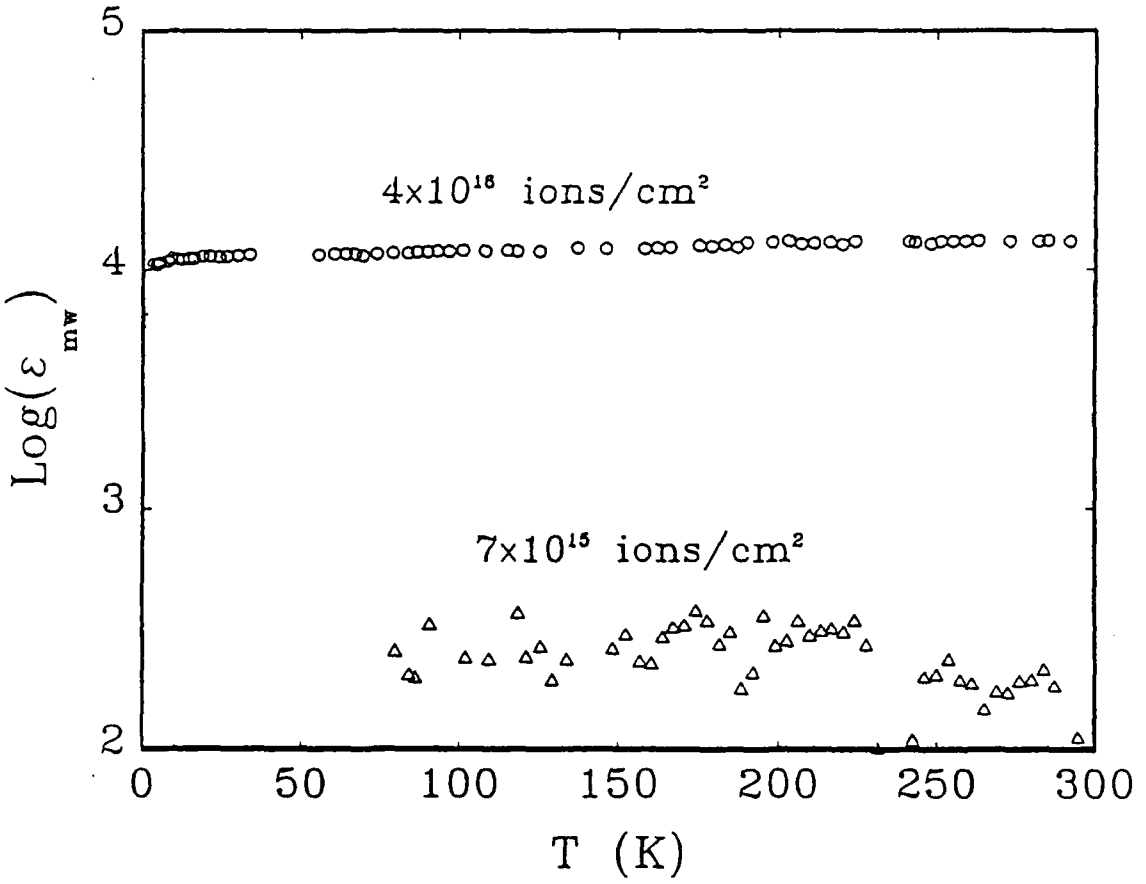

Figure 23 Microwave dielectric constant results of the lowest dosage (7×10^{15} ions/cm^2) PBO sample and a higher dosage (4×10^{16} ions/cm^2) sample.

Table 1. Effect of Annealing Temperature on the conductivity of implanted PBO, PBZT and BBL

	Normalized conductivity[a] $(\sigma_a/\sigma_{ua})_{RT}$		
T (^{0}C)	PBO	PBZT	BBL
~27	1.00	1.00	1.00
50	0.98	0.97	1.02
100	1.04	1.18	0.96
150	0.94	0.98	0.91
200	1.07	1.10	0.90
250	1.06	1.19	1.08
300	1.08	1.19	1.15
400	1.17	1.20	0.92

a. Conductivity of the annealed (σ_a) normalized with the conductivity of the unannealed (σ_{ua}) sample at room temperature.

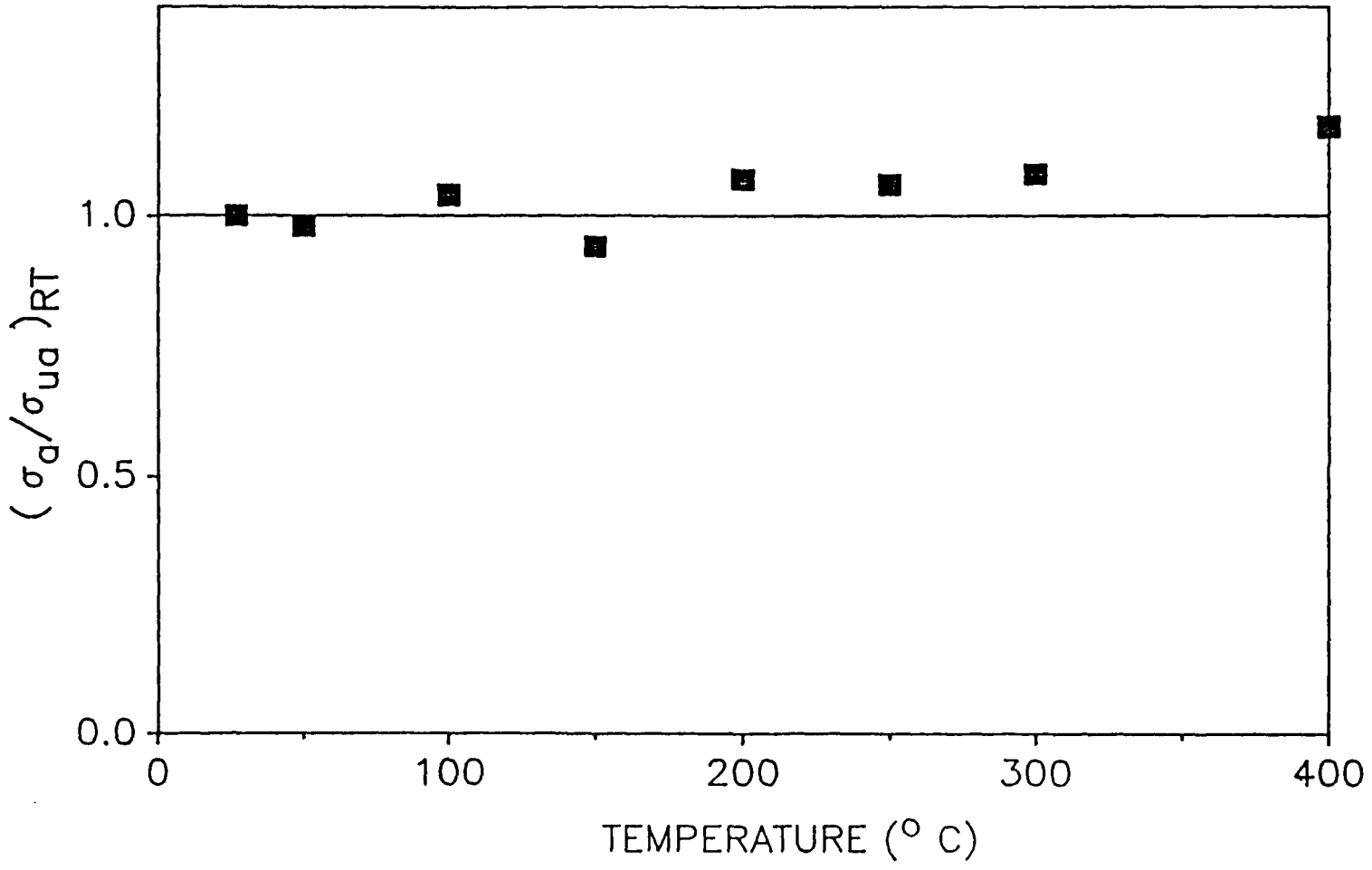

Figure 24 Effect of annealing temperature on room temperature conductivity of $^{84}Kr^{+}$ implanted PBO.

result in a more drastic and stable change in the structure, morphology and physical properties of these rigid-rod and ladder polymers. This observed stability of the physical properties (mechanical, thermal and electrical conductivity) with temperature and time is an important factor in the ultimate utilization of implanted materials in various technology applications.

II. B. vi Summary of Studies of Implanted Rigid Rod and Ladder Polymers

The charge transport mechanisms of the new group of strong and stable ion implanted polymers, PBO, PBT and BBL were systematically studied. Results of XPS, SEM, dc conductivity, thermopower, magnetoresistance, microwave conductivity, microwave dielectric constant, electron paramagnetic resonance, and Faraday susceptibility together yield a self-consistent picture of the new conducting state induced in the polymer as a function of implantation dosage. At higher dosage level ($\phi > 4 \times 10^{16}$ ions/cm^2) a semi-metallic state exists at higher temperatures (T > 30K). This conclusion is supported by the following experimental results:

-A flat optical absorption band, similar to that of disordered metals.

-A weakly temperature dependent conductivity with a room temperature value ~ 10^2 S/cm. This result is very different from that of the earlier studied implanted systems which showed strongly localized transport behavior. The result is fitted to the localization and e-e interaction model in the weakly localized regime. The fitting yields a finite conductivity at zero temperature for the data above 30 K.

-A small and positive magnetoconductance. Both magnetoconductance and dc conductivity results indicate that the localization and e-e interaction effects exist in this temperature region.

-A small and linearly *T*-dependent thermopower, which is usually observed in metallic materials.

-A large positive microwave frequency dielectric constant, which is also often observed in highly conducting materials.

However, this state is not truly metallic because the temperature dependent conductivity and the magnetoconductance results strongly suggest the application of the weak localization and e-e interaction model, which deals with an electron system just on the metallic side of a metal-insulator transition. By this theory, the electron conduction is determined by various types of scattering under the influence of the localization of electronic states. The charge transport in this semi-metallic state is not by electron hopping or tunneling which is the transport mechanism dominant in most chemically doped conducting polymers.[29]

The transport studies of three implanted polymers at the same ion dosage $\phi = 4 \times 10^{16}$ ions/cm^2 yielded surprisingly consistent results among the three materials. This suggest that the semi-metallic state in these implanted polymers is independent of the original chemical structure. According to the XPS, Raman studies and chemical characterization, such as the gas evolution during the implantation process and the color change after the process, we determined that the implantation process drives the heteroatoms out of the implanted layer. Thus, another conclusion of this study is that after the implantation, the original chemical structure is transformed into a disordered carbon network which is probably graphite-like. The similar transport properties shown among all three implanted materials suggest that the three original chemical structures have similar carbon backbone networks so the transformed carbon networks behave accordingly. The saturation of the metallic behavior reflected in the change in conductivity with increasing ion dosage indicates a 'maximum' carbon network (no more heteroatoms can be driven out) and the Fermi 'gas' in these systems reaches its extreme and will not grow further (at ion dosage $\phi \sim 10^{17}$ ions/cm^2).

More surprisingly, independent of starting rigid rod or ladder polymer, all the transport properties showed a consistent change in their behavior at $T_C \sim 30$ K, indicating a metal-non-metal transition with decreasing temperature at T_C. In summary, below T_C:

-The thermopower changes to a $1/T$ - dependent behavior, which is a semiconducting behavior. The hopping mechanisms in variable range hopping models are ruled out.

-The dc conductivity data deviate from the theoretical fitting curve and decrease more rapidly with decreasing T. This indicates that the finite zero temperature conductivity in the high temperature region does not hold as a constant in this low temperature region.

-The magnetoconductance changes its sign to negative which suggest a disappearance of the localization effect in this low T region. Thus, e-e interactions dominate in this region.

-Changes in the temperature behavior in both microwave dielectric constant and ESR susceptibility are present at ~ 30 K. These changes, together with the proposed decrease in σ_0, indicates a collapse of $N(E_F)$.

It is proposed from this study that the enhancement of e-e interactions at low temperatures, as a result of increased localization effect (which reduces Coulomb screening), results in a depletion in the DOS at the Fermi level, *i.e.* the opening of a Coulomb gap. Thus this Coulomb gap opens up in the weakly localized regime. We have seen the opening of a Coulomb gap on both sides of a MIT, so it is logical that such a gap can open in a region near a MIT. However, we lack a theoretical understanding of the effect of such a gap on the transport behavior in this situation. On the other hand, there might be other explanations for such a metal-non-metal transition. We consider this problem a challenge for the theorists.

When the ion dosage in the implantation process is varied, an insulator to metal transition occurs with increasing dosage. The transition occurs at $\phi \sim 4 \times 10^{16}$ ions/cm^2. This transition appears to be an Anderson transition in which the Fermi energy level is moved, passing the mobility edge in to the extended state region, upon increasing ion dosage. The changing of E_F is a result of increasing electron 'gas' created by the ion bombardment. The increase of the electron gas comes to a halt at $\phi \sim 10^{17}$ cm^{-2}, and the metallic behavior starts to saturate.

The critical dosage sample (4×10^{16} ions/cm^2) indeed showed a critical conductivity as expected near a metal to insulator transition. The sample with a dosage 7×10^{15} ions/cm^2 just below the critical dosage suggested a hopping or tunneling transport. However, the temperature dependence in

conductivity of this low dosage sample is rather complicated, because no single model describes the whole temperature range. The date analysis shows that a change in conductivity from $\sigma(T) \alpha \exp(-(T_0/T)^{1/2})$ to $\sigma(T) \alpha \exp(-(T'_0/T))$ occurs with decreasing T at 60 K. Although it is suggestive to explain this phenomenon in terms of a Coulomb gap again, the deviation in the characteristic parameter in this model suggests its inapplicability. Other relevant models do not work well either. Further theoretical investigation is needed.

II. B. vii Questions Remaining

The charge transport study of these ion implanted polymers revealed interesting phenomena in these materials. We understand some of them. But there are several questions which still remain.

-The application of the weak localization and e-e interaction model works well for the dc conductivity and magnetoconductance results. Usually, these effects are observed in semi-metallic systems at low temperatures.[23-25] The model is in good agreement with the dc conductivity data up to room temperature. This obvious difference between these materials and other semi-metallic systems needs to be understood.

-The Coulomb gap has been observed in insulating materials. The size of such a gap is usually less than 1 meV.[30] The transition in our systems occurs at ~ 30 K, which is about 2.6 meV. This proposed gap opens in the weakly localized regime in these implanted polymers. According to the usual theory, the gap in this regime should be smaller than that in the insulating regime. So, the value 2.6 meV is too large.

Despite these discrepancies, this study provides guiding facts and insights into these problems which will help in future studies.

II.C. References

1. R.L. Van Duesen, *J. Polym. Sci. Polym. Lett.* **B14,** 211 (1966).
2. F.E. Arnold and R.L. Van Duesen, *Macromolecules,* **2,** 49 (1969).
3. F.E. Arnold and R.L. Van Duesen, *J. Appl. Polym. Sci.* **15,** 2035 (1971).
4. F.E. Arnold , *J. Poly. Sci._Part A-1* **8,** 2079 (1970).
5. A.J. Sicree, F.E. Arnold, and R.L. Van Duesen, *J. Polym. Sci.: Polym. Chem. Ed.* **12,** 265 (1974).
6. J.F. Wolfe in: *"Encyclopedia of Polymer Science and Engineering,"* **11,** 2nd ed., John Wiley: New York, p. 601, (1988).
7. J.F. Wolfe and F.E. Arnold, *Macromolecules* **14,** 909 (1981); J.F. Wolfe, B.H. Boo, and F.E. Arnold, *Macromolecules* **14,** 915 (1981).
8. T.E. Helminiak, Preprints, *Am. Chem. Soc. Div. Org. Coat. Plast.* **40,** 475 (1979); T.E. Helminiak and F.E. Arnold, C.L. Benner, *Polym. Preprints* **16,** 659 (1975).
9. D.R. Ulrich, *Polymer* **28,** 533 (1987).
10. P.M. Hergenrother, *"Heat-Resistant Polymers"* in: *"Encyclopedia of Polymer Science and Engineering,"* **7,** 2nd ed., John Wiley: New York, p. 639 (1985).
11. P.E. Cassidy, *"Thermally Stable Polymers"*, Marcel Dekker: New York, (1980).
12. T.D. Dang, L.S. Tan, K.H. Wei, H.H. Chuah, and F.E. Arnold, *Polym. Mater. Sci. Eng.* **60** 424 (1989).
13. H. Mazurek, D.R. Day, E.W. Maby, J.S. Abel, S.D. Senturia, M.S. Dresselhaus, and G. Dresselhaus, *J. Poym. Sci. Polym. Phys. Ed.* **21,** 537 (1983).
14. G.E. Wnek, B. Wasserman, M.S. Dresselhaus, S.E. Tunney, and J.K. Stille, *J. Polym. Sci.: Polym. Lett. Ed.* **23,** 609 (1985).
15. S.A. Jenekhe and S.J. Tibbetts, *J. Polym. Sci: Polym. Phys. Ed.* **26,** 201 (1988).
16. H. A. Mizes and E. M. Conwell, *Phys. Rev. Lett.* **70,** 1505 (1993).
17. P. Vogl and D.K. Campbell, *Phys. Rev. Lett.* **62,** 2012 (1989).
18. D.D.C. Bradley, *Synth.Met.* **54,** 401 (1993), and references therein.
19. F. Coter, Y. Belaish, D. Davidov, L.R. Dalton, E. Ehrenfreund, M.R. McLean, and H.S. Nalwa, *Synth. Met.* **29,** E471 (1989).
20. B. Du, Bull, *Bull. Am. Phys. Soc.* **38,** 662 (1993).
21. G. Du, Z.H. Wang, A. Burns, J. Joo, J.A. Osaheni, S.A. Jenekhe, and A. J. Epstein, submitted.

22. S. Jasty, A.J. Epstein, J.A. Osaheni, S.A. Jenekhe, and C.S. Wang, *Bull. Am. Phys. Soc.* **38**, 238 (1993).
23. P.A. Lee and T.V. Ramakrishnan, *Rev. Mod. Phys.* **57**, 287 (1985), and references therein.
24. For a review, see A.L. Efros and M. Pollack, eds., *Electron-Electron Interactions in Disordered Systems, Elsevier, North Holland*, 1985.
25. For a review, see S. Kobayashi and F. Komori, Prog. Theor. Phys. Suppl. **84**, 224 (1985); Y. Ootuka and A. Kawabata, *ibid.* **84**, 249 (1985).
26. P,S, Vincent, W.A. Barlow, R.A. Hann, and G.G. Roberts, *Thin Solid Films* **94**, 171 (1982); **94**, 476 (1982).
27. C. Adachi, S. Tokito, T. Tsutsui, and S. Saito, *Jpn. J. Appl. Phys.* **27**, L713 (1988).
28. C.S. Wang, J. Burkett, C.Y.C. Lee, and F. E. Arnold, *Polym. Mater. Sci. Eng.* **64**, 171 (1991).
29. H.H.S. Javadi, A. Chakraborty, C. Li, N. Theophilou, D.B. Swanson, A.G. MacDiarmid, and A.J. Epstein, *Phys. Rev. B* **43**, 2183 (1991); Z.H. Wang, A. Ray, A.G. MacDiarmid, and A.J. Epstein, *Phys. Rev. B* **43**, 4373 (1991); Z.H. Wang, C. Li, E,M. Scherr, A.G. MacDiarmid, and A.J. Epstein, *Phys. Rev. Lett.* **66**, 1745 (1991); and, Z.H. Wang, E.M. Scherr, A.G. MacDiarmid, and A.J. Epstein, *Phys. Rev. B* **45**, 4190 (1992).
30. I. Shlimak, M. Kaveh, and M. Yosefin, *Phys. Rev. Lett.* **68**, 3076 (1992).

III. CUMULATIVE LIST OF WRITTEN PUBLICATIONS PUBLISHED, SUBMITTED, AND IN PREPARATION

1. A. Burns, Z.H. Wang, G. Du, J. Joo, A.J. Epstein, J.A. Osaheni, S.A. Jenekhe, and C.S. Wang, *Ion Implantation of Conducting Ladder and Rigid-Rod Polymers,* **Mat. Res. Soc. Symp. Proc. 247**, 735-740 (1992).

2. J.A. Osaheni, S.A. Jenekhe, A. Burns, G. Du, J. Joo, Z.H. Wang, A.J. Epstein, H. Song, and C.S. Wang, *Spectroscopic and Morphological Studies of Highly Conducting Ion-Implanted Rigid-Rod and Ladder Polymers* , **Macromolecules 25**, 5828-5835 (1992).

3. G. Du, Z.H. Wang, A. Burns, J. Joo, J.A. Osaheni, S.A. Jenekhe, and A.J. Epstein, *Anomalous Metal-Non-Metal Transition in Ion-Implanted Polymers,* Submitted to **Physical Review B, Rapid Communications.**

4. G. Du, A. Burns, J. Joo, Z.H. Wang, J.A. Osaheni, S.A. Jenekhe, and A.J. Epstein, *Charge Transport Study on Ion-Implanted Ladder and Rigid-Rod Polymers: Electron Localization and Coulomb Interaction,* Manuscript in Preparation for **Physical Review B.**

5. S. Jasty, J.A. Osaheni, S.A. Jenekhe, and A.J. Epstein, *Magnetic Susceptibility of Ion-Implanted Polymers: Effects of Localization and Metal-Non-Metal Transition,* Manuscript in Preparation for **Physical Review B.**

6. K.S. Narayan, S.M. Long, J.A. Osaheni, S.A. Jenekhe, and A.J. Epstein, *Transport and EPR Studies of Heat-Treated Ladder Polymers,* Manuscript in Preparation for **Physical Review B.**

7. A. Burns, R. Kohlman, R.M. McCall, J.A. Osaheni, S.A. Jenekhe, and A.J. Epstein, *Photo-Induced Absorption Studies of Ladder Polymers,* Manuscript in Preparation for **Physical Review B.**

8. K.S. Narayan, A.J. Epstein, J.A. Osaheni, S.A. Jenekhe, and C.S. Wang, *Temperature Dependent Photoconductivity Studies of Ladder Polymers,* Manuscript in Preparation for **Physical Review B.**

IV.a. PROFESSIONAL PERSONNEL ASSOCIATED WITH RESEARCH EFFORT

The Ohio State University

Postdoctoral Fellows

Andrew Burns (79%)

K.S. Narayan (71%; At Wright Patterson Air Force Base)

R.M. McCall (14%)

Shashi Jasty (7%)

Graduate Students

Jinsoo Joo (50%)

Gang Du (32%)

Randolph Kohlman (11%)

Kimberly Coplin (9%)

Stephen Long (7%)

Kwangjoon Kim (7%)

University of Rochester

Graduate Students

John A. Osaheni (75%)

IV.b. ADVANCED DEGREES AWARDED

The Ohio State University

Recipient: Gang Du

Degree: Ph.D. (Physics)

Date: Summer 1993 (Anticipated)

Thesis Title: "*Electron-Electron Interaction and Localization in Ion-Implanted Polymers*"

Recipient: Jinsoo Joo

Degree: Ph.D. (Physics)

Date: Fall 1993 (Anticipated)

Thesis Title: "*Charge Delocalization in Conducting Polymers*"

V.a. PAPERS PRESENTED AT MEETINGS, CONFERENCES, AND SEMINARS

1. Z.H. Wang, A. Burns, J.S. Joo, A.J. Epstein, C.S. Wang, J.A. Osaheni, and S.A. Jenekhe, *Transport Properties of Ion-Implanted Ladder and Rigid Rod Conducting Polymers,* **Materials Research Society Fall Meeting,** Boston, Massachusetts, 2-6 December 1991 (paper N11.36).

2. A. Burns, R. P. McCall, G. Du, J. Joo, A.J. Epstein, C.S. Wang, *Infrared and Photoinduced Infrared Studies of Rigid Rod and Ladder Polymers,* **American Physical Society 1992 March Meeting,** Indianapolis, Indiana, 16-20 March 1992 [Bulletin of the American Physical Society **37,** 505 (1992)].

3. G. Du, Z.H. Wang, A. Burns, J. Joo, A.J. Epstein, S.A. Jenekhe, J.A. Osaheni, C.S. Wang, *Charge Transport in Ion-Implanted Polymers,* **American Physical Society 1992 March Meeting,** Indianapolis, Indiana, 16-20 March 1992 [Bulletin of the American Physical Society **37,** 569 (1992)].

4. J. Joo, Z.H. Wang, G. Du, A. Burns, A.J. Epstein, J.A. Osaheni, S.A. Jenekhe, C.S. Wang, *High Microwave Dielectric Constants of Ion-implanted Polymers,* **American Physical Society 1992 March Meeting,** Indianapolis, Indiana, 16-20 March 1992 [Bulletin of the American Physical Society **37,** 724 (1992)].

5. G. Du, J. Joo, A. Burns, Z. Wang, S. Jasty, P. Zhou, S.A. Jenekhe, J.A. Osaheni, C.S. Wang, and A.J. Epstein, *Weak Localization, Electron-Electron Interaction, and Metal-Insulator Transition in Ion-Implanted Polymers*, **International Conference on Science and Technology of Synthetic Metals**, Göteborg, Sweden, 12-18 August 1992.

6.* G. Du, *Coulomb Interactions and Metal-Insulator Transition in Ion-Implanted Polymers*, **American Physical Society 1993 March Meeting,** Seattle, Washington, March 21-26, 1993 [Bulletin of the American Physical Society **38,** 662 (1993)].

7. K.S. Narayan, S.M. Long, A.J. Epstein, B.E. Taylor, R.J. Spry, S.J. Bai and C.S. Wang, *Photoconductivity and Thermally Induced Effects in Polybenzimidazobenzophenanthroline (BBL)*, **American Physical Society 1993 March Meeting**, Seattle, Washington, March 21-26, 1993 [Bulletin of the American Physical Society **38** ,110 (1993)].

8. G. Du, J. Joo, A. Burns, A. J. Epstein, S.A. Jenekhe, and J.A. Osaheni, *Ion Dosage Dependence of Metal-Insulator Transition for Ion-Implanted Polymers*, **American Physical Society 1993 March Meeting**, Seattle, Washington, March 21-26, 1993 [Bulletin of the American Physical Society **38**, 238 (1993)].

9. S. Jasty, A.J. Epstein, J.A. Osaheni, and S.A. Jenekhe, *Magnetic Susceptibility of Ion-Implanted Polymers: Effects of Disorder and Electron-Electron Interaction*, **American Physical Society 1993 March Meeting**, Seattle, Washington, March 21-26, 1993 [Bulletin of the American Physical Society **38**, 238 (1993)].

* Invited Talk

V.b. CONSULTATIVE AND ADVISORY FUNCTIONS TO OTHER LABORATORIES AND AGENCIES

1. Presentation at the AFOSR Polymer Blend Contract Review, 2 April 1993, Air Force Academy, Colorado Springs, Colorado, entitled:
"Electrical Conductivity of Ion Implanted Ladder Polymers"

The program was organized and chaired by Dr. Charles Y-C Lee (AFOSR) and attended by:

R. Lescanec (for N. Thomas, MIT)
F. Bates (U. of Minnesota)
R. Lad (for W. Unertl, U. Maine)
H. Reiss (UCLA)
I. Sanchez (U. Texas - Austin)
M. Connolly (for F. Karasz, U. Mass.)
S. Kumar (Georgia Tech)
G. Berry (Carnegie Mellon U.)

VI. NEW DISCOVERIES, INVENTIONS, OR PATENT DISCLOSURES AND SPECIFIC APPLICATIONS STEMMING FROM THE RESEARCH EFFORT

Section II provides a summary of the significant accomplishments during this program. We have found that ion implantation of rigid rod, ladder and single ladder polymers leads to a new state of carbon-based matter which is thermally stable, environmentally stable and sufficiently highly conducting to be usable for circuitry and contacts for many applications. We have discovered that this ion implanted carbon system has a novel insulator to metal transition as a function of ion dosage and, for high dosage levels, as a function of temperature. No patent disclosures were submitted based on this work.

VII. OTHER STATEMENTS

In sum, we have carried out an integrated program of chemical characterization, structural characterization, conductivity, electron spin resonance, microwave conductivity and dielectric constant, magnetotransport, thermopower, and direct and photoinduced spectroscopy of pristine and ion implanted rigid rod, pseudo ladder and ladder polymers. These integrated efforts have demonstrated that these thermally and environmentally stable materials can be converted to a highly conducting state with novel electronic properties. These materials are now poised for examination of their potential application in areas as diverse as electroluminescent devices and photoconductive devices based upon the optoelectronic properties of the insulating polymer and use of the conducting properties of the ion-implanted polymers for contacts.